AD-A147 970 TWO-DIMENSIONAL MODELING FOR LINEAL AND AREAL PROBABILITIES OF WEATHER CONDITIONS(U) AIR FORCE GEOPHYSICS LAB HANSCOM AFB MA C F BURGER ET AL. 1/1

UNCLASSIFIED 10 APR 84 AFGL-TR-84-0126 F/G 4/2 NL

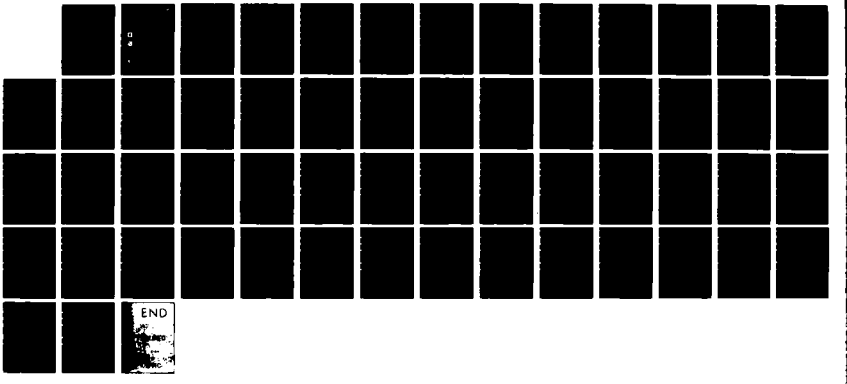

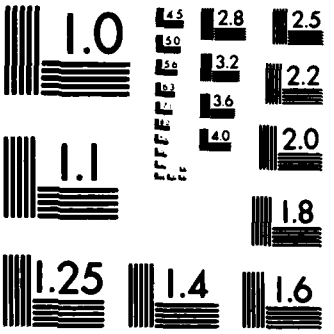

AFGL-TR-84-0126
ENVIRONMENTAL RESEARCH PAPERS, NO. 875

12

Two-Dimensional Modeling for Lineal and Areal Probabilities of Weather Conditions

CHARLES F. BURGER
IRVING I. GRINGORTEN

10 April 1984

ATMOSPHERIC SCIENCES DIVISION PROJECT 6670
AIR FORCE GEOPHYSICS LABORATORY
HANSCOM AFB, MA 01731

This report has been reviewed by the ESD Public Affairs Office (PA) and is releasable to the National Technical Information Service (NTIS).

"This technical report has been reviewed and is approved for publication"

FOR THE COMMANDER

DONALD D. GRANTHAM
Chief, Tropospheric Structure Branch

ROBERT A. McCLATCHEY
Director, Atmospheric Sciences Division

Qualified requestors may obtain additional copies from the Defense Technical Information Center. All others should apply to the National Technical Information Service.

If your address has changed, or if you wish to be removed from the mailing list, or if the addressee is no longer employed by your organization, please notify AFGL/DAA, Hanscom AFB, MA 01731. This will assist us in maintaining a current mailing list.

Do not return copies of this report unless contractual obligations or notices on a specific document requires that it be returned.

Unclassified

SECURITY CLASSIFICATION OF THIS PAGE

REPORT DOCUMENTATION PAGE

1a. REPORT SECURITY CLASSIFICATION Unclassified	1b. RESTRICTIVE MARKINGS
2a. SECURITY CLASSIFICATION AUTHORITY	3. DISTRIBUTION/AVAILABILITY OF REPORT Approved for public release; distribution unlimited.
2b. DECLASSIFICATION/DOWNGRADING SCHEDULE	
4. PERFORMING ORGANIZATION REPORT NUMBER(S) AFGL-TR-84-0126, ERP No. 875	5. MONITORING ORGANIZATION REPORT NUMBER(S)
6a. NAME OF PERFORMING ORGANIZATION Air Force Geophysics Laboratory 6b. OFFICE SYMBOL (If applicable) LYT	7a. NAME OF MONITORING ORGANIZATION
6c. ADDRESS (City, State and ZIP Code) Hanscom AFB Massachusetts 01731	7b. ADDRESS (City, State and ZIP Code)
8a. NAME OF FUNDING/SPONSORING ORGANIZATION 8b. OFFICE SYMBOL (If applicable)	9. PROCUREMENT INSTRUMENT IDENTIFICATION NUMBER
8c. ADDRESS (City, State and ZIP Code)	10. SOURCE OF FUNDING NOS. PROGRAM ELEMENT NO.: 62101F; PROJECT NO.: 6670; TASK NO.: 09; WORK UNIT NO.: 10
11. TITLE (Include Security Classification) (U) Two-Dimensional Modeling for Lineal and Areal (over)	
12. PERSONAL AUTHOR(S) Burger, Charles F., and Gringorten, Irving I.	
13a. TYPE OF REPORT Scientific 13b. TIME COVERED FROM _____ TO _____	14. DATE OF REPORT (Yr., Mo., Day) 1984 April 10 15. PAGE COUNT 58
16. SUPPLEMENTARY NOTATION	

17. COSATI CODES			18. SUBJECT TERMS (Continue on reverse if necessary and identify by block number)	
FIELD	GROUP	SUB. GR.		
		0402	Monte Carlo simulation	Cumulative probability distribution
			Boehm Sawtooth Wave model	
			Equivalent Normal Deviate	Correlation coefficient

19. ABSTRACT (Continue on reverse if necessary and identify by block number)

Single-point probabilities of weather conditions, which are easily estimated from climatic records, have been extended to lines and areas by means of Monte Carlo simulation. Simulation was accomplished using the Boehm Sawtooth Wave (BSW) model. This model was chosen because of its speed and simplicity, and because it has a spatial correlation function similar to that of many weather elements. The BSW model generates fields (or maps) of normally distributed values called Equivalent Normal Deviates (ENDs). The procedure was to obtain the cumulative probability distribution for threshold END values. To do this, a large number of maps had to be generated, 25,000 in all, to approximate the true probability distributions. This was done for 12 different-sized square areas and lines. The results were put in graphical form by plotting the probabilities as a function of areal and lineal size, and fitting them to curves through hand analysis. The curves were then fitted by equations, making it possible to obtain solutions quickly by computer. Thus, a model has been produced that can be used to

20. DISTRIBUTION/AVAILABILITY OF ABSTRACT UNCLASSIFIED/UNLIMITED ☒ SAME AS RPT. ☒ DTIC USERS ☐	21. ABSTRACT SECURITY CLASSIFICATION Unclassified
22a. NAME OF RESPONSIBLE INDIVIDUAL Charles F. Burger	22b. TELEPHONE NUMBER (Include Area Code) (617) 861-5956 22c. OFFICE SYMBOL LYT

DD FORM 1473, 83 APR EDITION OF 1 JAN 73 IS OBSOLETE.

Unclassified

SECURITY CLASSIFICATION OF THIS PAGE

Block 11 (contd)
Probabilities of Weather Conditions

Block 19 (contd)

estimate the probability that a certain weather condition will cover a given area or length, or fraction of an area or length. Examples explain in detail how to use the graphs and equations. The model results are approximate, depending upon the effectiveness of the BSW model, and the degree of accuracy of the Monte Carlo process, the smoothed analysis, and the fit of the equations. The model must be tested over a period of time to determine how well it works and to determine its strengths and weaknesses.

Contents

Illustrations

Tables

Two-Dimensional Modeling for Lineal and Areal Probabilities of Weather Conditions

1. INTRODUCTION

The single-point probability of a weather condition is easily estimated from climatic records. The extension of single-point probabilities to a line or an area is often necessary but difficult to obtain, as in studies of rainfall coverage and cloud-free lines-of-sight. If the probability is known, say, of 24-hour rainfall exceeding 10 mm at a single observational point, we must ask: what is the corresponding probability that the same quantity will be exceeded everywhere in a surrounding area or in some fraction of a surrounding area? This type of climatology is the subject of this paper.

In general, efforts to describe the areal and lineal coverage of weather conditions have been few, and models of areal and lineal coverage have been rare. In most previous studies, correlation coefficients are the principal object of investigation, with several notable exceptions. Schreiner and Riedel[1] collected rainfall data integrated over areas ranging in size from 26 km^2 to 2600 km^2, and have found frequencies of extremes of rainfall as a function of size of the ground

(Received for publication 11 April 1984)

1. Schreiner, L.C., and Riedel, J.F. (1978) Probable maximum precipitation estimates United States east of 105th meridian, Hydrometeorol. Report (No. 51), NOAA-NWS-HR-51.

covered. Other studies, by Court,[2] Roberts,[3] and Briggs[4] have linked the rain in a circular area to the central single-station amounts by idealized models. Jones and Wendland[5] used data from arrays of instantaneous-precipitation intensity recorders to obtain line averages of the frequency of exceedence of threshold precipitation intensities. Gringorten[6] describes Model B, which was devised by a method that produces a simulated horizontal field, stochastically, without recourse to physical laws or dynamics. Many such random fields were generated, then summarized, and the results graphed so that the probabilities of fractional coverages of events along lines or in areas of different sizes could be estimated.

Theoretically, an abundance of data at an abundance of stations in a small area, with a rapid succession of observations, could provide the kind of areal climatology that we seek. Practically speaking, such abundance, if it really existed, would confront us with the enormous task of mapping and recording events to provide a history of the weather before summarizing it statistically. Since such a climatology would be regionally dependent and applicable only to the weather element being studied, we would have to repeat the task for each new area and/or meteorological parameter of interest. These are the difficulties we wish to overcome by modeling. We want to be able to simulate a sequence of changes in the weather covering an area whenever and wherever we choose. In addition, we want, ultimately, to provide usable statistics of areal coverage, including correlation coefficients and probabilities of fractional cover by any type of weather condition, such as cloud cover.

A model of the areal extent of the weather can resemble a Markov process, but it cannot be one. In a Markov model, a future event is dependent upon the present state of the weather, and its likelihood is not directly affected by previous events. In a horizontal picture, any one point is surrounded in all directions by

---

2. Court, A. (1961) Area-depth rainfall formulas, J. Geophys. Res. 66:1823-1831.
3. Roberts, C.F. (1971) A note on the derivation of a scale measure for precipitation events, Mon. Wea. Rev. 99:873-876.
4. Briggs, J. (1972) Probability of aircraft encounters with heavy rain, Meteorol. Mag. 101:8-13.
5. Jones, D.M.A., and Wendland, W.M. (1983) Statistics of Instantaneous Rainfall Rates, AFGL-TR-83-0056, AD A130089.
6. Gringorten, I.I. (1979) Probability models of weather conditions occupying a line or an area, J. Appl. Meteorol. 18:957-977.

an infinite number of points. Consequently, there must be some underlying restraint on the conditions surrounding that point, similar to, but still different from, a Markov process.

An effective model of areal coverage will produce a simulated horizontal field, stochastically, without recourse to physical laws or dynamics, as in Gringorten's Model B.[6] In our approach, we use such stochastic, or Monte Carlo, simulation to obtain graphical solutions. We make two major improvements over Gringorten's original Model B approach. First, we have fitted the graphs by equations, an accomplishment that is a major step in areal and lineal probability modeling. It is now possible to obtain solutions quickly from the computer instead of reading them from graphs. Second, we have replaced Gringorten's Model B with a more recent development, Boehm's Sawtooth Wave model (BSW), as described in Section 3. The two primary reasons for choosing BSW over Model B are: First, the spatial correlation of the BSW output is closer to reality than that of the Model B, and, second, the new model requires the generation of only a few dozen random numbers per map instead of many thousands, as required for Model B. This increase in model efficiency has enabled the generation of a greater sampling size, given the same computer limitations.

2. EQUIVALENT NORMAL DEVIATE (END)

Before introducing the model, we must examine the concept of the equivalent normal deviate (END). Figure 1 is a sample plot of the cumulative frequency of a weather element, in this case of visibility (V) at Bedford, Mass., in January, at noontime. The X's mark the frequencies that have been summarized from 20 years of data. They show, for example, a 2 percent frequency for V less than one-fourth of a mile, 7 percent for V less than 1 mile, and 38 percent for V less than 10 miles, or, alternately, a 62 percent frequency of V greater than 10 miles. Alongside the scale of cumulative probability, we can plot another scale of the equivalent normal deviate (y). The correspondence of y to F(y) can be found in nearly every textbook on statistics. Using either a diagram such as Figure 1, or equations, we obtain a transformation of the variable (V in this case) into its END (y), or vice versa, through the cumulative probability of the variable (V).

Our models are derived using the ENDs. We then transform the results to the appropriate weather variables.

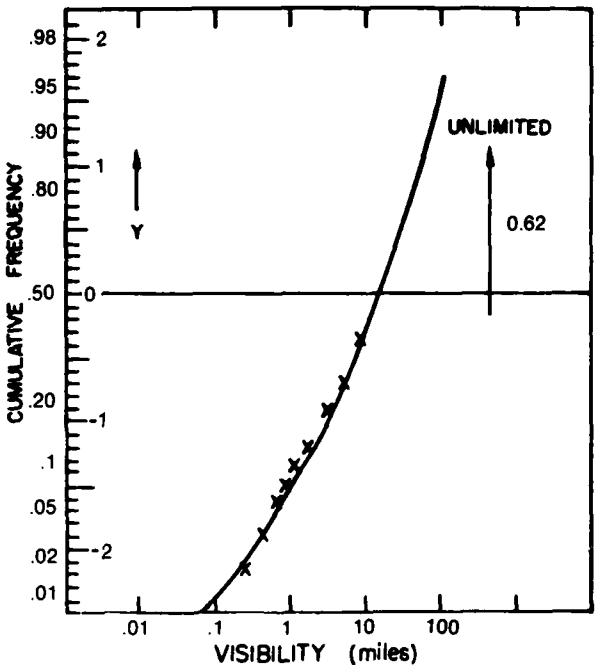

Figure 1. Plot of Cumulative Frequency of Visibility (V) at Bedford, Mass., in January at Noontime

3. BOEHM'S SAWTOOTH WAVE MODEL (BSW)

The present model was devised by Major Albert R. Boehm, USAFETAC, Scott AFB, Ill. He has given it the descriptive name Sawtooth Wave. The following is a brief overview of the model:

A cross-sectional view of the sawtooth waves is shown in Figure 2. The waves are stationary. The lefthand edge of each wave has zero height; the right-hand edge has a height of unity. At any point in between, a wave has a uniformly distributed height (H) between 0 and 1. The goal is to use the sawtooth waves to generate fields of the normally distributed values, ENDs, which have a mean of 0 and a variance of 1.

Now consider a formation of sawtooth waves in horizontal space, uniform in wavelength (Λ), such as the one shown in Figure 3. Each diagonal line represents the leading edge of a wave, with the height of each wave increasing toward the upper right. The wavelength is a parameter of the model, which, in our climatic fields, measures several hundred to several thousand kilometers. For derivation, the wavelength is made the unit of distance. The positioning of the wave

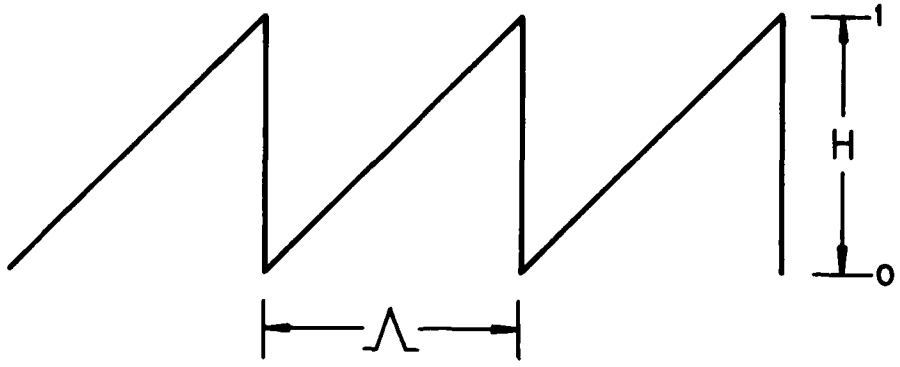

Figure 2. Cross-Sectional View of Sawtooth Waves

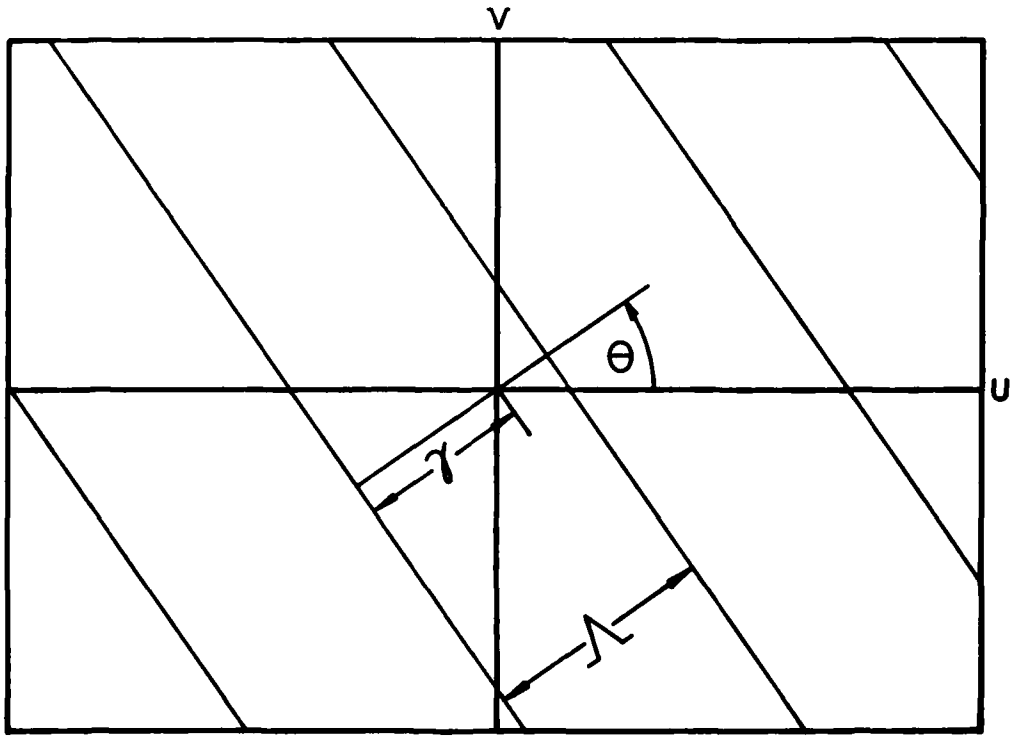

Figure 3. Formation of Sawtooth Waves in Horizontal Space

formation about the u, v axis and point of origin (0, 0) is determined by two numbers. One, the angle θ, gives the orientation of the wave formation ($0 \leq \theta < 2\pi$); the other, γ, determines the wave phase at the point of origin ($0 \leq \gamma < 1$). Once the wave formation has been positioned, there is a wave height (H) at each point (u, v). H is between 0 and 1.

Simulation is accomplished by randomly choosing many (N) pairs of θ and γ values, thereby positioning N random wave formations. Then, at each (u, v), there are N values of H(u, v). A number y(u, v) is calculated at each (u, v) from the sum of the N values of H(u, v) as follows,

$$y(u, v) = \sqrt{\frac{12}{N}} \left(\sum_{n=1}^{N} H_n(u, v) - \frac{N}{2} \right). \tag{1}$$

As N increases, by the central limit theorem, the values of y(u, v) approach the normal distribution, and hence y becomes an END. A sample of a field of ENDs generated by BSW is shown in Figure 4. The isopleths are labeled in terms of y = -2(1)1.

4. CORRELATION AND SCALE PARAMETER

An analytical solution has been found for BSW for the correlation coefficient $\rho(s)$ between points separated by distance (s), in units of the wavelength:

$$\rho(s) = 1 - \left(\frac{12}{\pi}\right) s + 3s^2 \qquad \text{for } 0 \leq s \leq 1 \tag{2}$$

$$= 1 - \left(\frac{12}{\pi}\right) s + 3s^2 + (24/\pi) \left[\cos^{-1}(1/s) - \sqrt{s^2 - 1}\right] \qquad \text{for } 1 < s \leq 2.$$

The derivation of Eq. (2) is given in Appendix A. The graph of $\rho(s)$ versus s is shown in the top half of Figure 5. For our purposes, we shall rarely need to consider distances of more than one or two wavelengths. The distance s, then, will usually be a number between 0 and 2, given by

$$s = s'/\Lambda, \tag{3}$$

where s' is the measured distance (km) and Λ is the wavelength (km). The top graph of Figure 5 compares favorably with the bottom graph, which is an example of the spatial correlation function of the winter surface temperature between

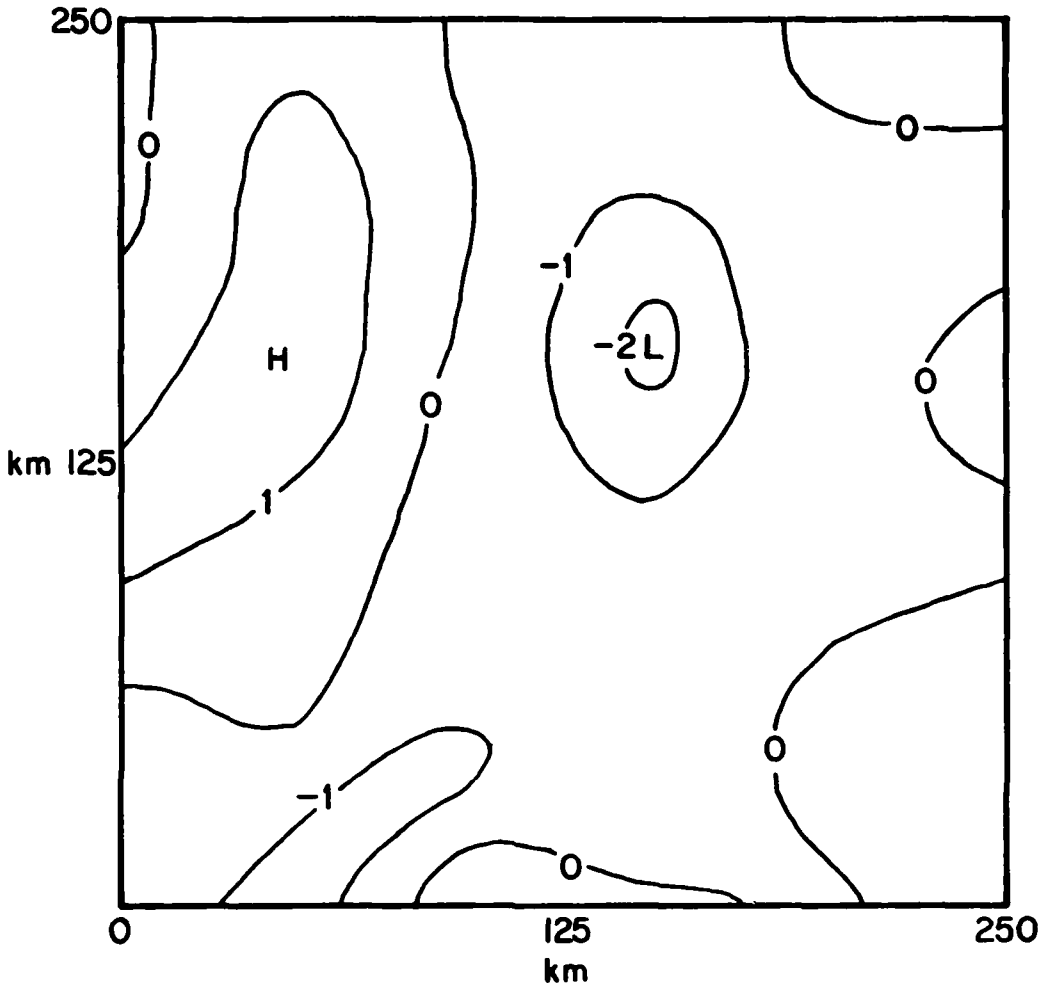

Figure 4. Example of Horizontal Field of ENDs Generated Stochastically by the BSW Model

stations from a few kilometers to several thousand kilometers apart taken from Bertoni and Lund.[7] This is an analysis made from actual observations. Correlation is high for short distances, but drops monotonically to zero and becomes negative at substantial distances between stations. Bertoni and Lund found that

7. Bertoni, E.A., and Lund, I.A. (1964) Winter space correlations of pressure, temperature and density to 16 km, Environ. Res. Papers (No. 75), AFCRL-64-1020, AD 611002.

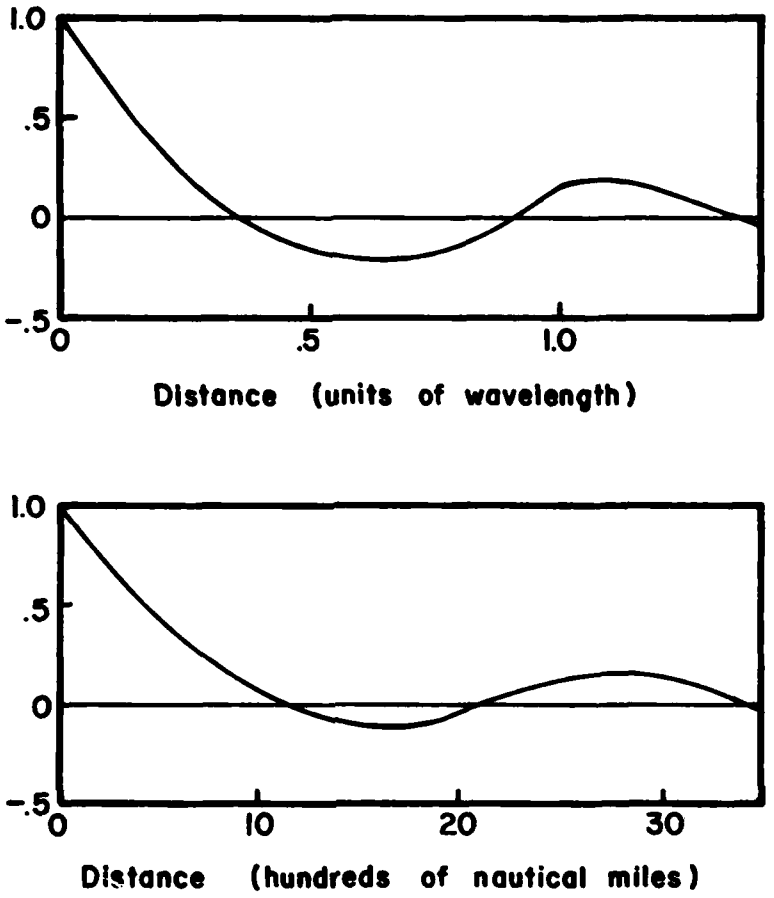

Figure 5. Distance Versus Correlation Coefficient for BSW Model (Top Graph) and for Winter Surface Temperature From Bertoni and Lund[7] (Bottom Graph)

this pattern of spatial correlation holds for temperature at different levels of the atmosphere up to at least 16 km, as well as for pressure and density at these levels. Eq. (2) yields $\rho(s)$ equal to 0.99 over a distance of 1 km, if $\Lambda \doteq 340$ km. This distance has been called the scale distance, r (km), and can be used interchangeably with the wavelength, Λ (km) as the parameter of the model. The ratio between the two alternatives is a constant, chosen for this paper to be 1/340. Thus

$$r = (\Lambda/340) \text{ km.} \tag{4}$$

5. LINEAL AND AREAL COVERAGE

Analytical solutions for the probability of the maximum condition in an area or a fraction of an area, or a line or fraction of a line, have not yet been found. Instead, we have obtained approximate solutions by Monte Carlo simulation. The following is a brief description of our procedure for the areal case.

Consider a square area of side s (in units of the wavelength) containing a field of ENDs generated by BSW, such as in Figure 4. At some point in the area (s^2) there will be a maximum value of y for the entire field. Also, there will be a minimum of the highest 10 percent of values, a minimum of the highest 20 percent, and finally the minimum for the entire field. This can also be stated in terms of the fraction (F/10) of the area covered: 10 percent, for which F = 1; 20 percent, for which F = 2, etc. Our goal is to find the cumulative probability distribution for each of these minimum or threshold values $[y(F, s)]$. A large number of stochastically generated maps will provide a frequency distribution that will approach the true probability distribution P(y; F, s) asymptotically as the number of maps is increased.

We conducted this kind of Monte Carlo simulation for 12 square areas of different sizes, where the linear side of each square, in units of wavelength, was

$$s = 2^z/\Lambda, \tag{5}$$

where z = -1(1)8. For this exercise, we chose Λ to be 340 km, so that $\rho(s)$ would be approximately 0.99 over a distance of 1 km (see Section 4). For each square, we generated 25,000 maps, and surveyed each map for the threshold values y(F, z). From each map, we found the (F)th decile of y(F, z) in the area (s^2) for F = 0(1)10. From all maps collectively, we found the cumulative frequencies for the 19 values of y(F, z) between -4.5(0.5)4.5, thus estimating the cumulative probabilities, P(y; F, z) for each of the 11 values of F and each of the 10 values of z. We drew curves to show P(y; F, z) as a function of y(F, z) and z, one graph for each value of F. The graphs for F = 0 through F = 5 are shown in Figures 6-11. Because the Monte Carlo method yields only an approximation of the true answer, we had to smooth the raw simulation data when drawing the curves. Smoothing was especially necessary at the extremes of the distributions, where very high and very low probabilities made the approximations noticeably less reliable because the simulations were limited to 25,000 maps. A typical example of the extent of the smoothing is shown in Figure 6a for F = 0, where the dots represent the raw data. In Figures 6b-11, the crosses do not represent the raw data, but represent approximations to the smoothed curves made by an empirical solution that will be described in Section 6. On the graphs, the horizontal axis has a uniform z-scale, and

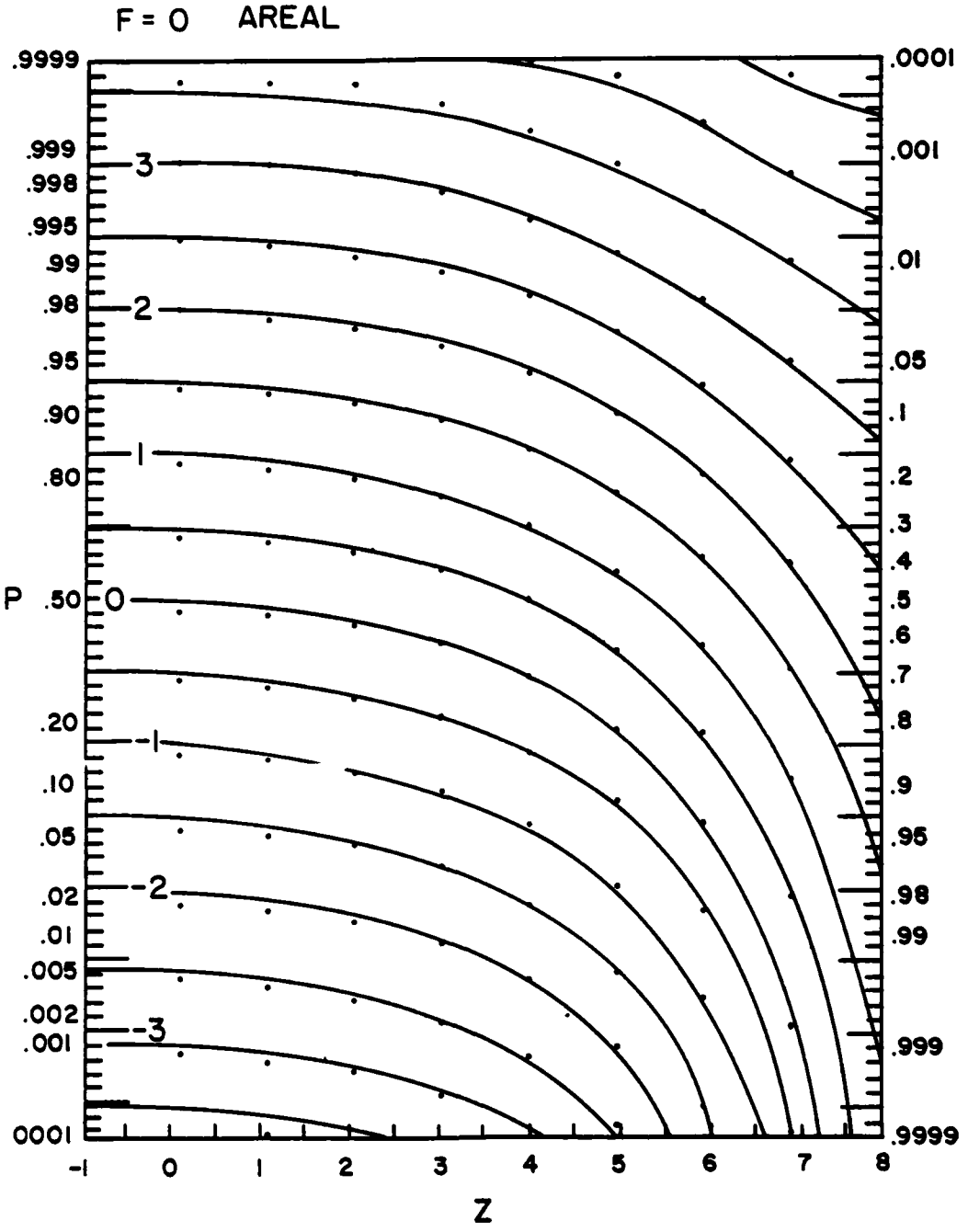

Figure 6a. BSW-Model Probability Estimates for 0/10 Areal Coverage for Area (s^2) Corresponding to z = ln s/ln 2. The lines represent the smoothed analyses, each corresponding to a single y_0-value, and the dots represent the Monte Carlo simulation data

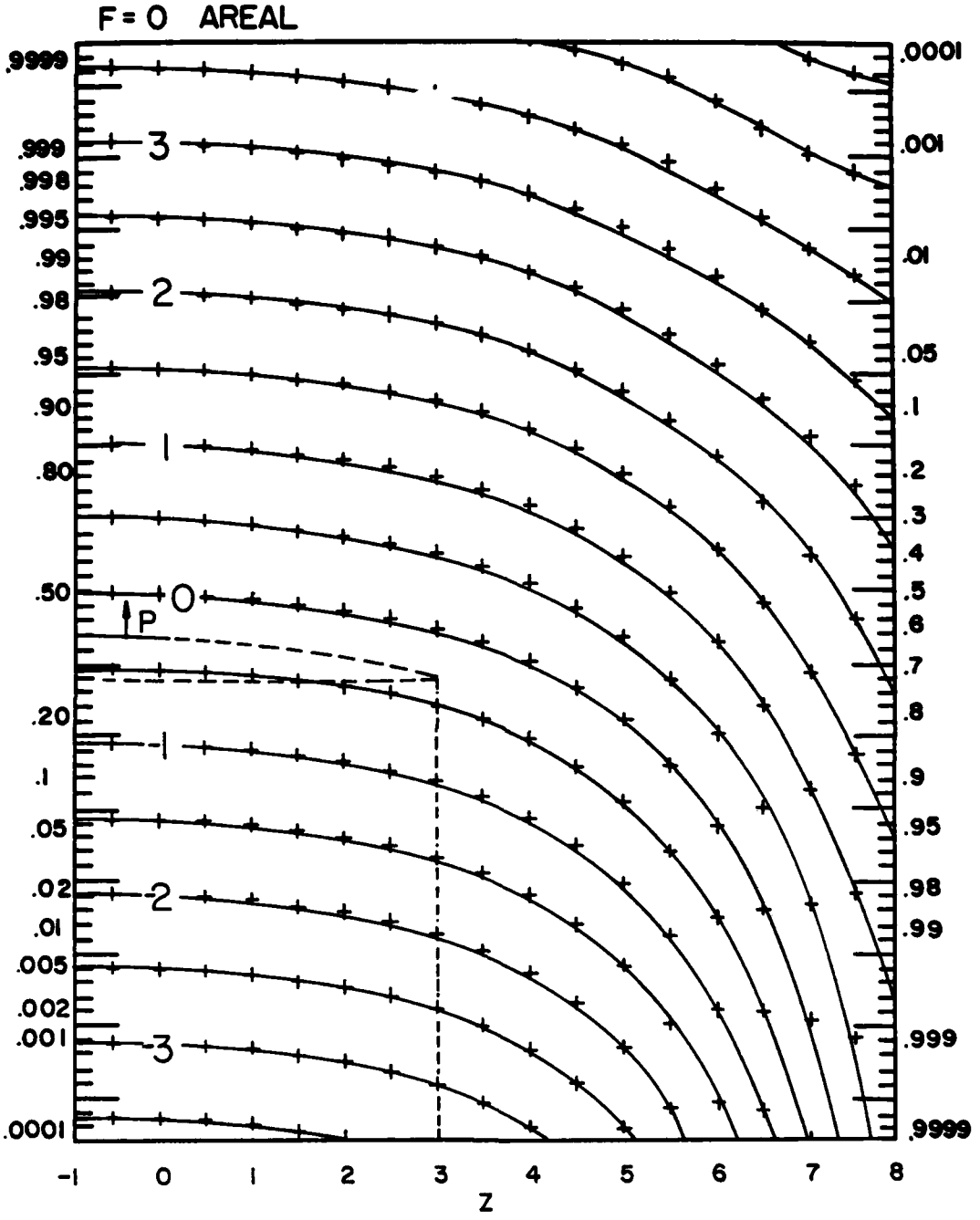

Figure 6b. BSW-Model Probability Estimates for 0/10 Areal Coverage for Area (s^2) Corresponding to z = ln s/ln 2. The lines represent the smoothed analyses, each corresponding to a single y_0-value, and the crosses represent the computer solutions

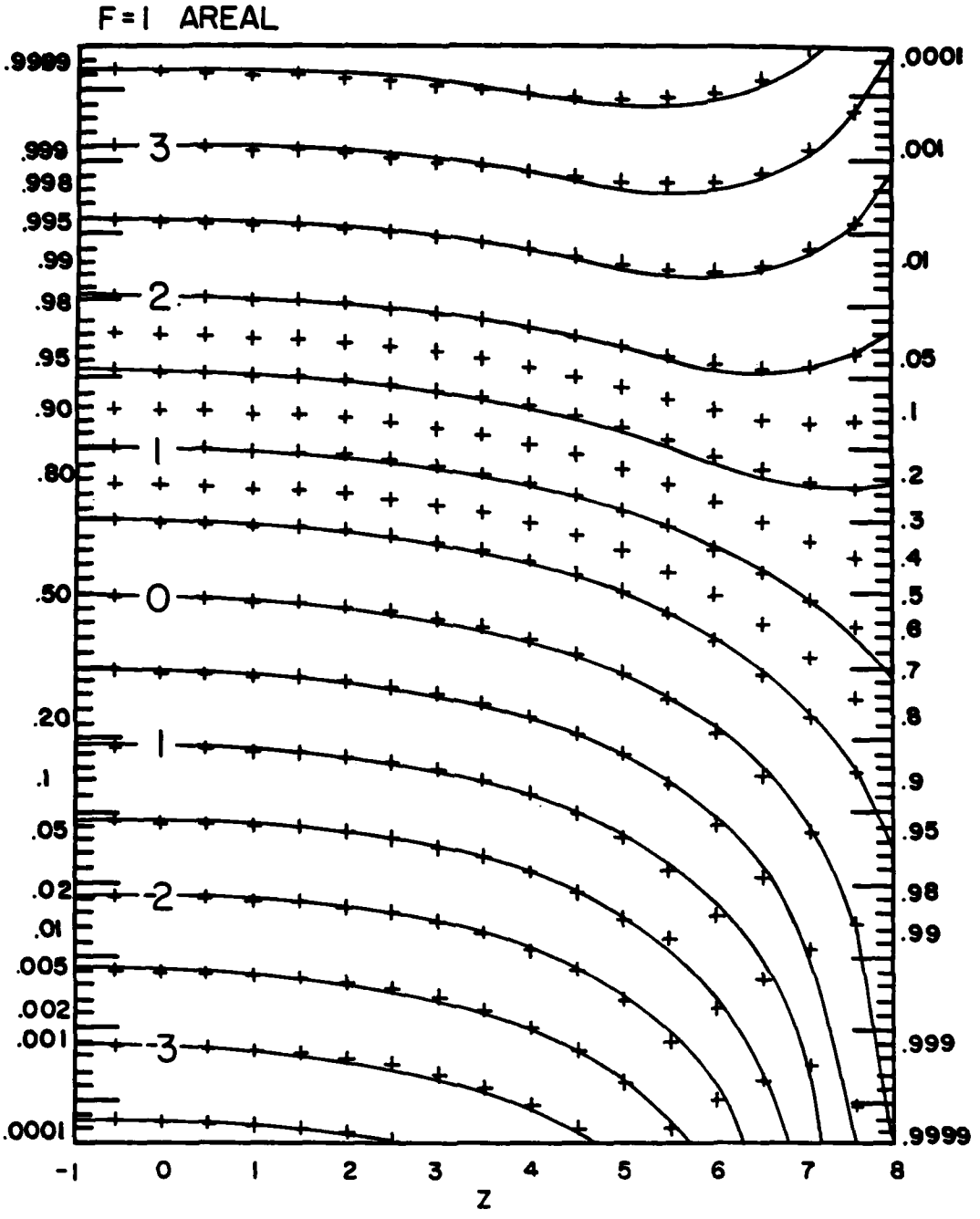

Figure 7. 1/10 or Less Areal Coverage for Area (s^2) Corresponding to z = ln s/-ln 2. The lines represent the smoothed analyses, each corresponding to a single y_0-value, and the crosses represent the computer solutions. Extra crosses are computer solutions for y_0 = 0.75, 1.25, and 1.75

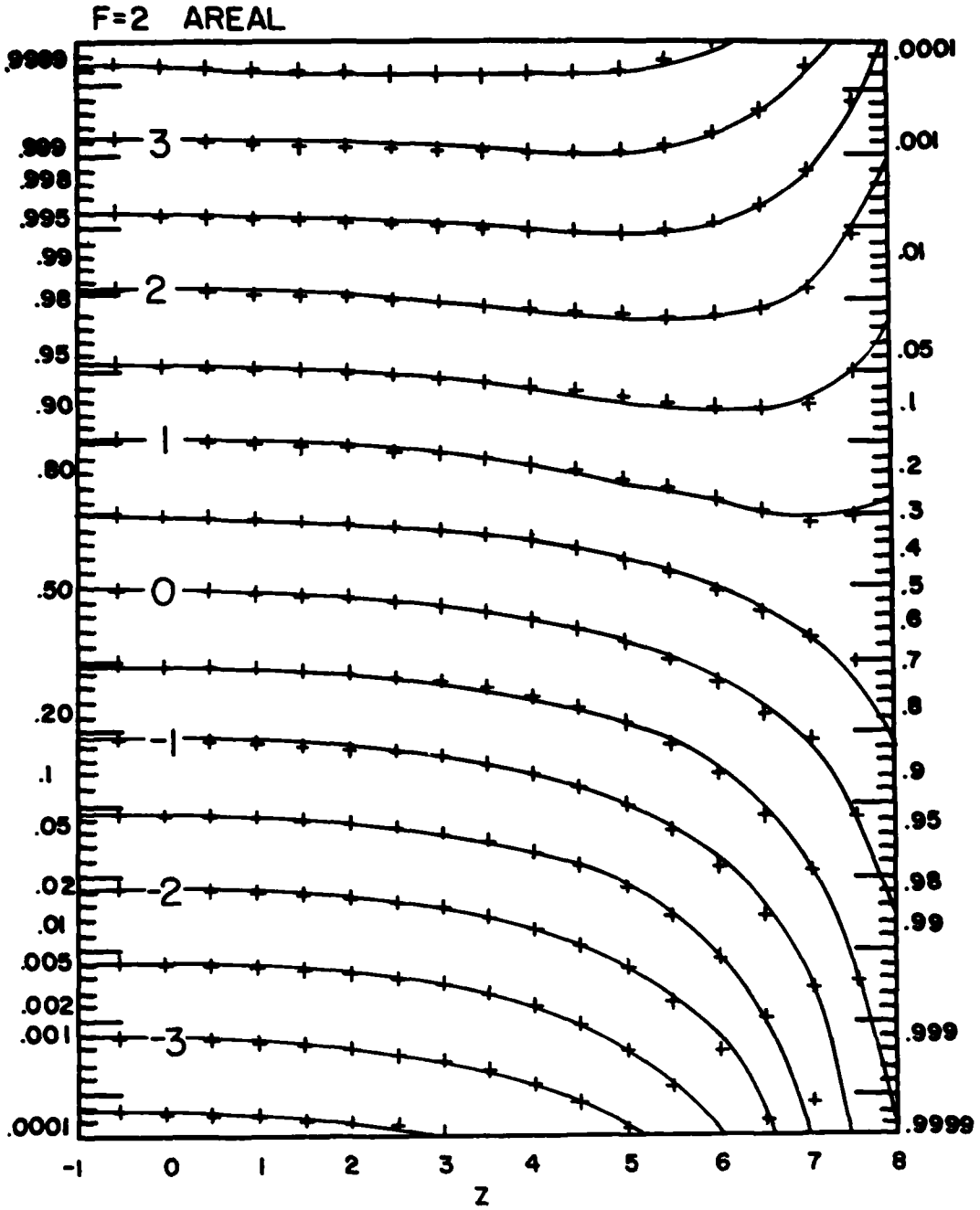

Figure 8. 2/10 or Less Areal Coverage for Area (s^2) Corresponding to $z = \ln s / -\ln 2$. The lines represent the smoothed analyses, each corresponding to a single y_0-value, and the crosses represent the computer solutions

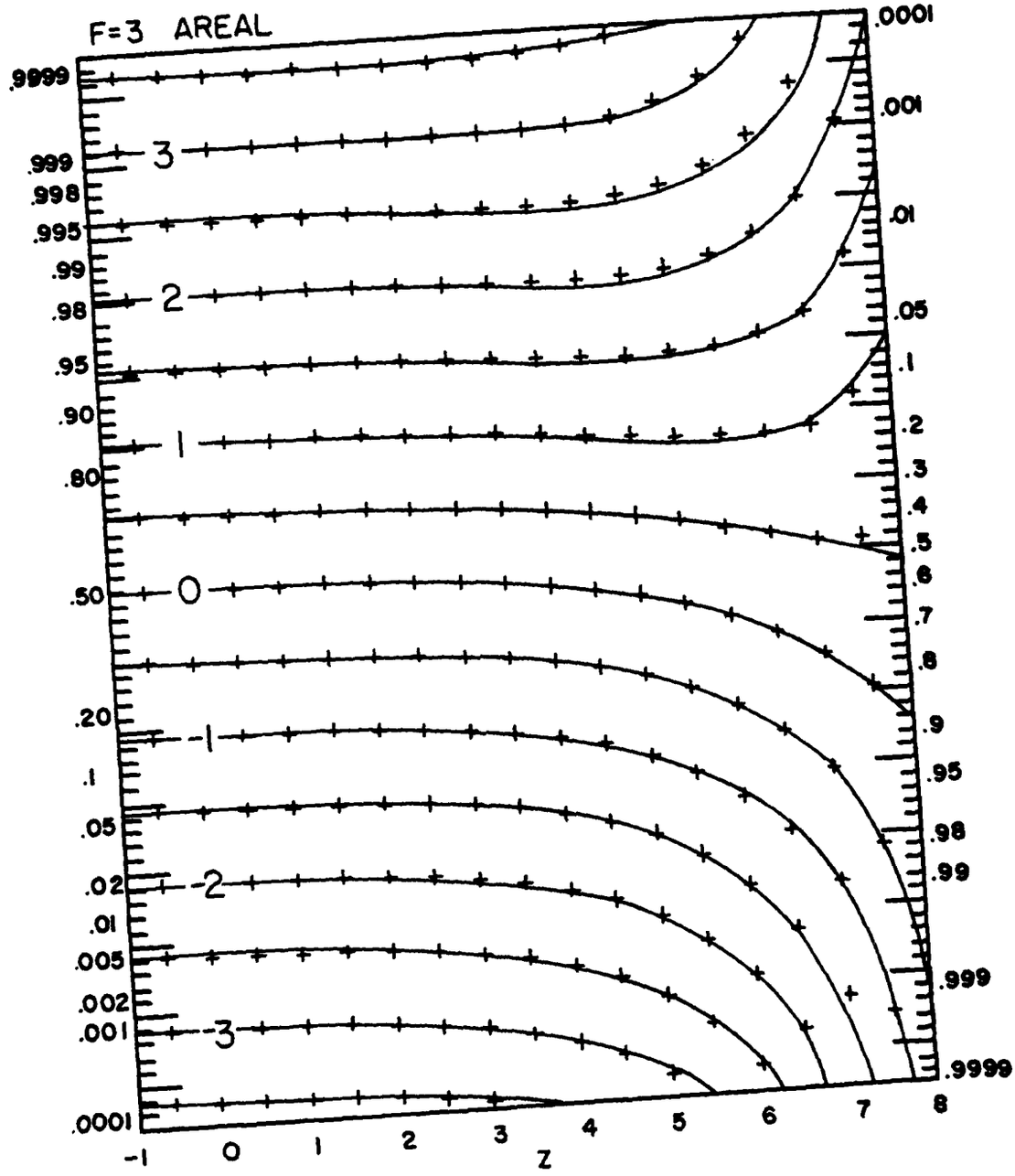

Figure 9. 3/10 or Less Areal Coverage for Area (s^2) Corresponding to $z = \ln s/-\ln 2$. The lines represent the smoothed analyses, each corresponding to a single y_0-value, and the crosses represent the computer solutions

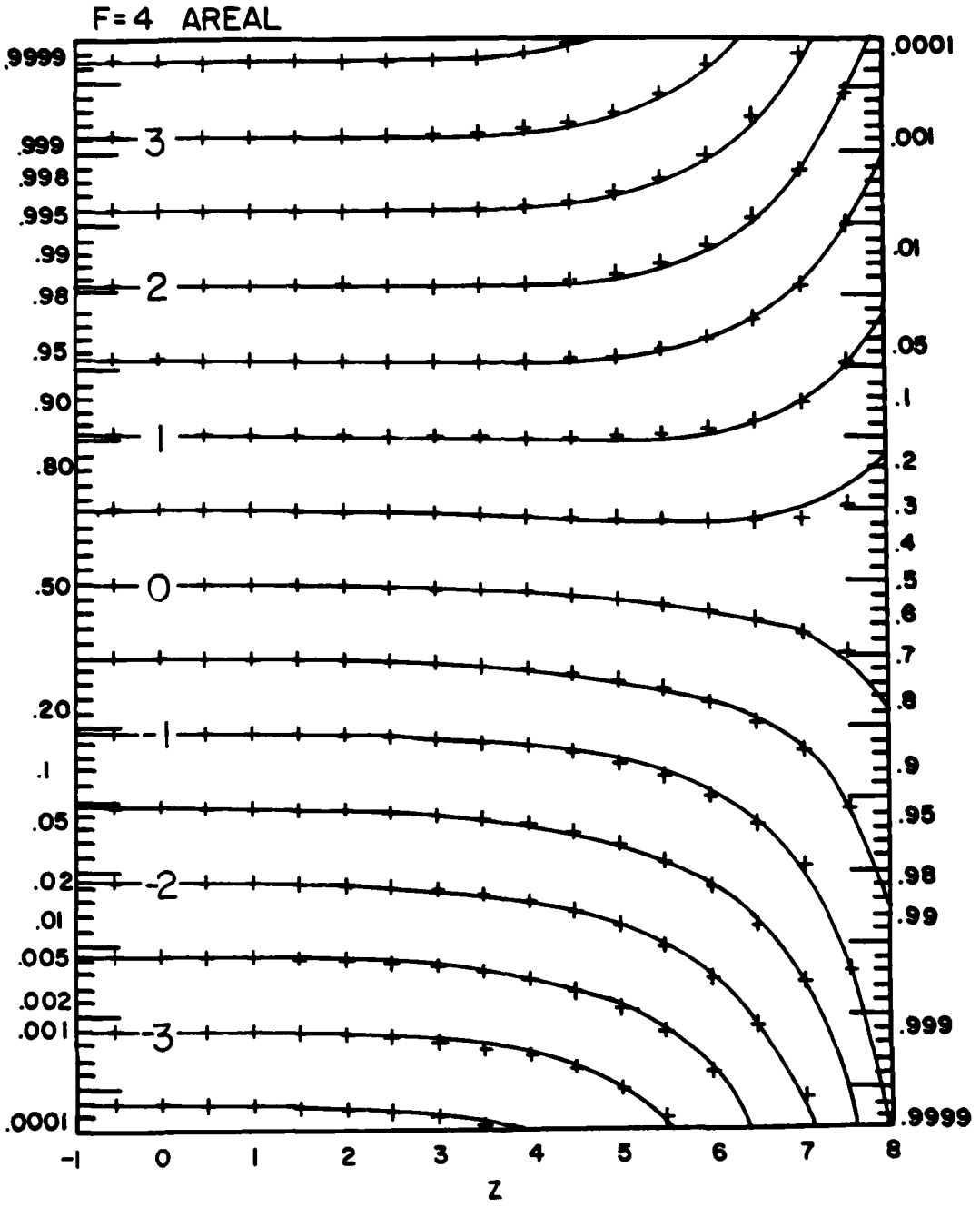

Figure 10. 4/10 or Less Areal Coverage for Area (s^2) Corresponding to z = ln s/ln 2. The lines represent the smoothed analyses, each corresponding to a single y_0-value, and the crosses represent the computer solutions

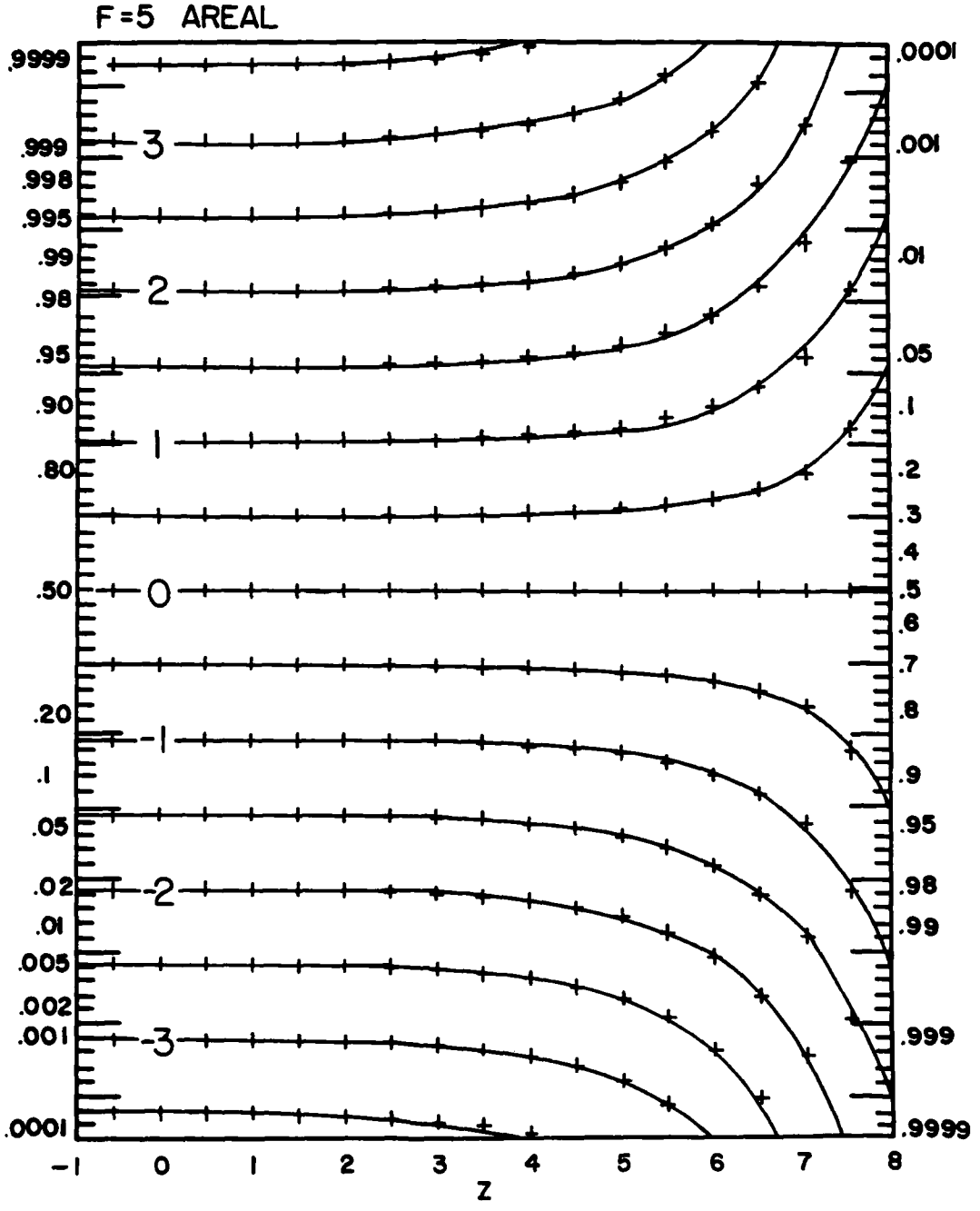

Figure 11. 5/10 or Less Areal Coverage for Area (s^2) Corresponding to z = ln s/ln 2. The lines represent the smoothed analyses, each corresponding to a single y_0-value, and the crosses represent the computer solutions

is therefore a logarithmic scale with respect to the area. The vertical axis is uniform in the END (y) of the cumulative probability (P). The graphs for F = 6 through F = 10 are not shown because they are merely the inverted mirror images of the graphs for F = 4 through F = 0, respectively. For inverted mirror images, one simply reverses the sign of y(F, z) and takes the complement of P(y; F, z). Each graph shows the value of P within the limits $0.0001 \leq P(y; F, z) \leq 0.9999$.

We obtained graphs of the probability of the maximum condition along a line or fraction of a line using the same procedure described above, with model values simulated along a line instead of over an area (Figures 12-17).

Thus far, this procedure has produced a model that can be used to estimate the probability that a certain weather condition will cover a given area or given length, or a fraction of an area or length. The input includes the single-point cumulative probability of the weather element (P'_0), the area or length of concern (A km^2 or s' km), and the parameter: either the scale distance (r km) or the wavelength (Λ km).

The scale distance, by and large, is a more meaningful parameter than the wavelength, although the ratio between the two is constant. In results obtained with New England 24-hour precipitation,[6] we found that the scale distance equals 9 to 10 km. For radar echoes, on a PPI-scope, the scale distance ranged from 1 - 3 km in summer to 2.5 - 4.5 km in winter.

In the graphs (Figures 6-17), the abscissa is in terms of z, where

$$z = \ln(\sqrt{A}/r)/\ln 2 \text{ for areas (A)}, \tag{6a}$$

$$z = \ln(s'/r)/\ln 2 \text{ for lines (s')}, \tag{6b}$$

from which we obtain

$$r = \sqrt{A}/2^z \tag{7a}$$

$$r = s'/2^z. \tag{7b}$$

To illustrate the operability of the graphs, suppose we examine a weather condition, such as visibility (V) less than 10 miles. For Bedford, in January at noontime (Figure 1), the single-point climatic frequency of visibility over 10 miles is $P_0 = 0.62$. The cumulative frequency is $P'_0 = 0.38$, for which the END is $y_0 = -0.30$. Each curve on the graphs corresponds to a y_0 - value. For an area of 1000 km^2 and scale distance of, say, 4 km, Eq. 6a gives $z \doteq 3$. When the curve (interpolated) for $y_0 = -0.30$ is followed to the vertical line for z = 3 on Figure 6b, for example, it gives the probability $P(V < 10; F=0, z=3) = 0.29$, as

shown by the dashed lines in the figure. Detailed instructions on practical applications of the graphs are given in Section 7.

6. EMPIRICAL ALGORITHMS

The graphs of $P(y_0 ; F, z)$ for the areal and lineal cases were fitted to empirical equations in terms of y_0, F, and z as follows:

$$y' = \alpha + \beta + \gamma + \delta \qquad \text{(areal)} \tag{8}$$

$$y' = \eta_1 + (\eta_2 - \eta_1)(F - \text{INT}(F)) \qquad \text{(lineal)} \tag{9}$$

where y' denotes the END of $P(y_0; F, z)$. The terms α, β, γ, and δ are given in Table 1 and the associated constants in Tables 2 and 3; the term η_i (i = 1 or 2) is given in Table 4, and the associated constants in Table 5. When F > 5, then $P(y_0; F, z) = 1 - P(-y_0; 10-F, z)$. In addition, in the areal case only, when z > 7, if F ≠ INT, then $y' = y'(\text{INT}(F)) + (F-\text{INT}(F))(y'(\text{INT}(F)+1) - y'(\text{INT}(F)))$.* These solutions are valid only within the bounds of the graphs, and therefore include the following restrictions: $|y'| \leq 3.72$, $|y_0| \leq 4.7$ and $-1 \leq z \leq 8$.

These formulas represent a major step in areal and lineal probability modeling, for it is now possible to obtain solutions with a computer as opposed to finding them in a graph. Previously, in the case of Gringorten,[6] only the graphs were available. Note, also, that the formulas allow for solutions for any value of F instead of just the integer values, as with the graphs. In other words, the empirical solutions interpolate between graphs, so that it is possible, for example, to use the model for eighths of cloud cover as well as tenths.

The goodness of the fit of these equations to the analyzed graphs can be determined both visually and objectively. The visual comparison is depicted in Figures 6b-11 for the areal graphs and Figures 12-17 for the lineal graphs, corresponding to F = 0 through F = 5 (0/10 through 5/10 areal/lineal coverage). The empirical formula was solved at regular intervals of z for the values of y_0 depicted by the solid lines. The solutions were plotted as shown by the crosses. The goodness of the fit of Eqs. (8) and (9) for graphs F = 6(1)10 is the same as the fit for graphs F = 0(1)4, since the former are upside-down mirror images of the latter. Visually, the fit is excellent. It is difficult to tell the difference between the original analyses and the computer solutions. Certainly, the error between the curves

*INT is a function that acts to truncate any number to its integer value.

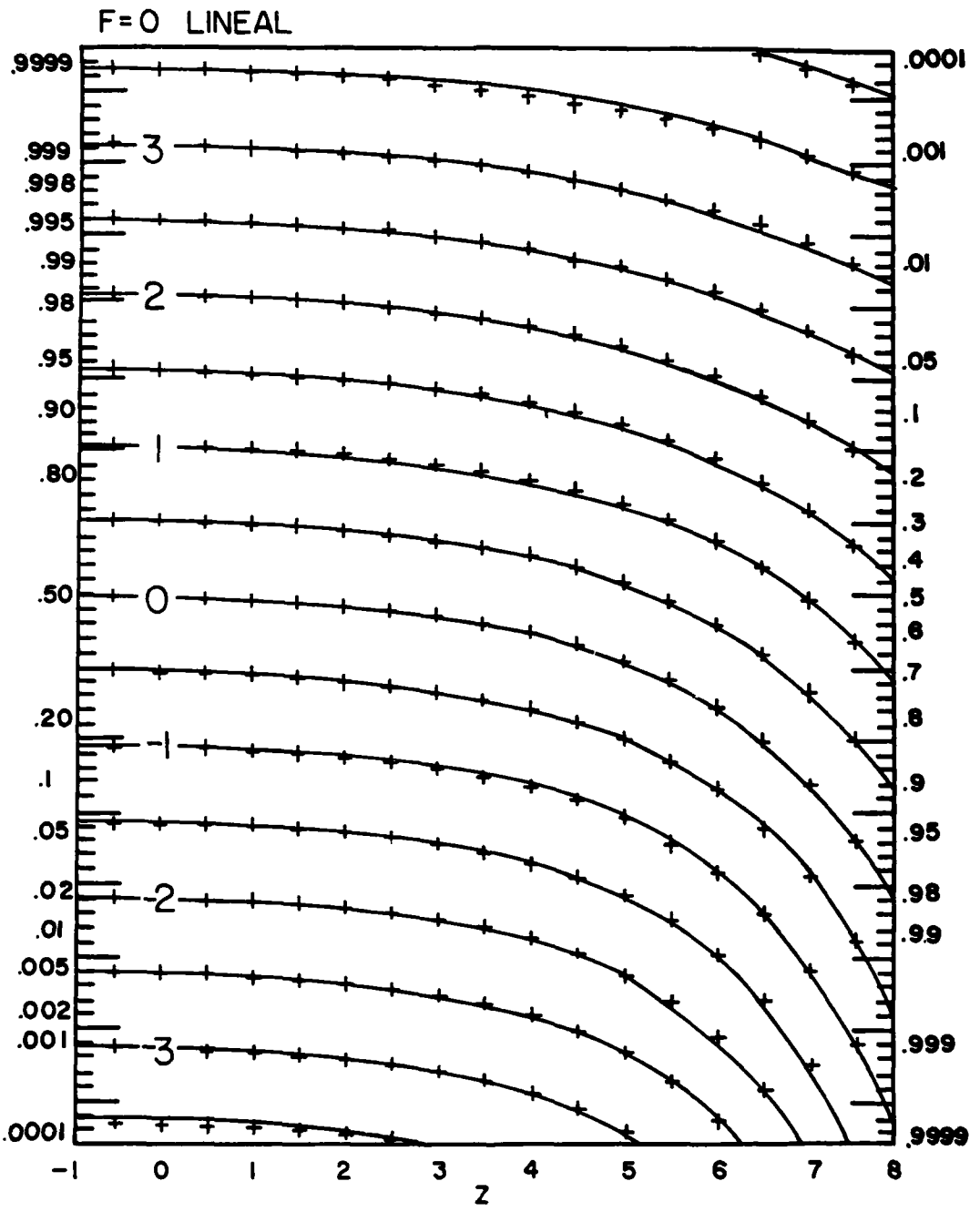

Figure 12. BSW-Model Probability Estimates for 0/10 Lineal Coverage for Length (s) Corresponding to z = ln s/ln 2. The lines represent the smoothed analyses, each corresponding to a single y_0-value, and the crosses represent the computer solutions

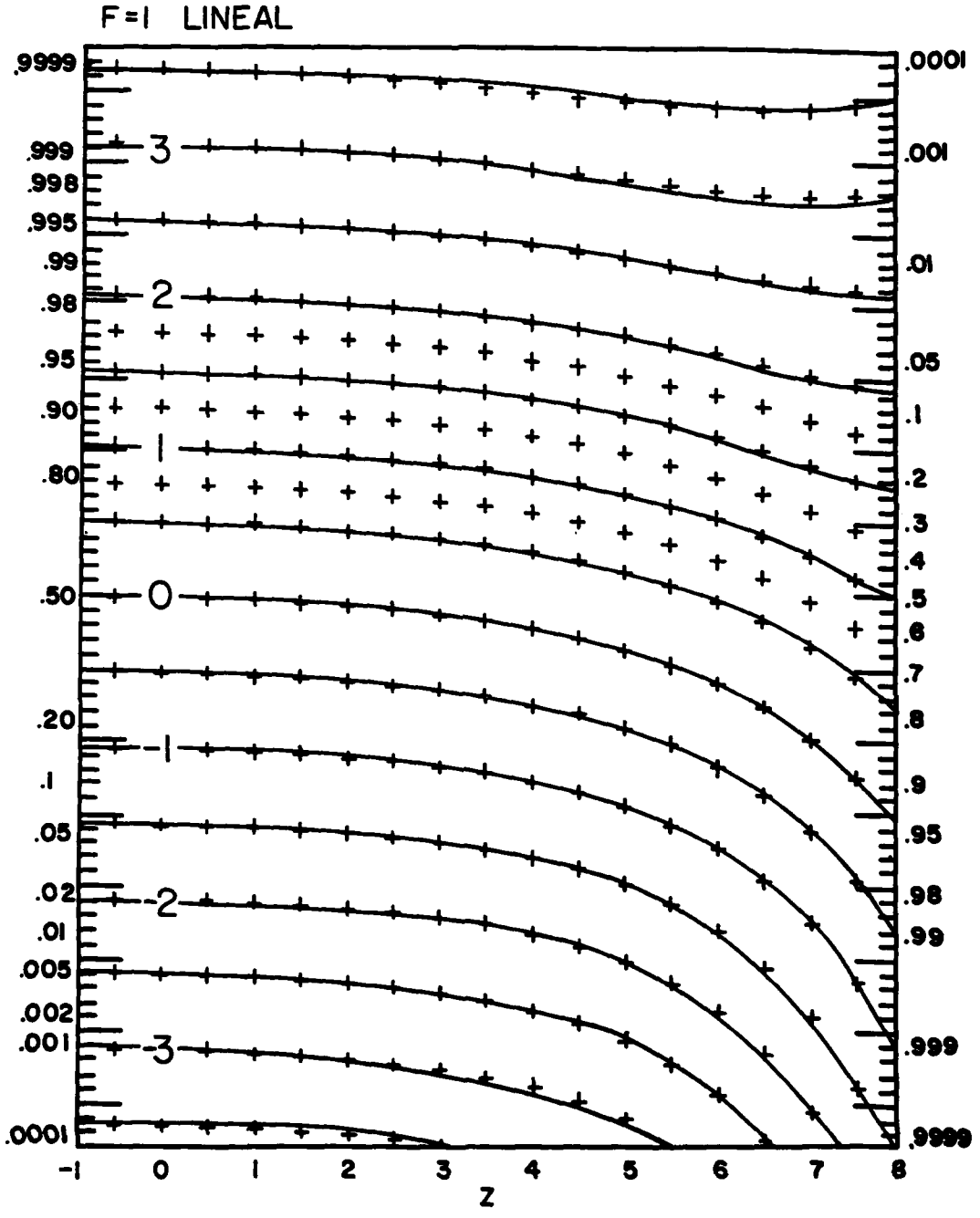

Figure 13. 1/10 or Less Lineal Coverage for Length (s) Corresponding to z = ln s/ln 2. The lines represent the smoothed analyses, each corresponding to a single y_0-value, and the crosses represent the computer solutions. Extra crosses are computer solutions for y_0 = 0.75, 1.25, and 1.75

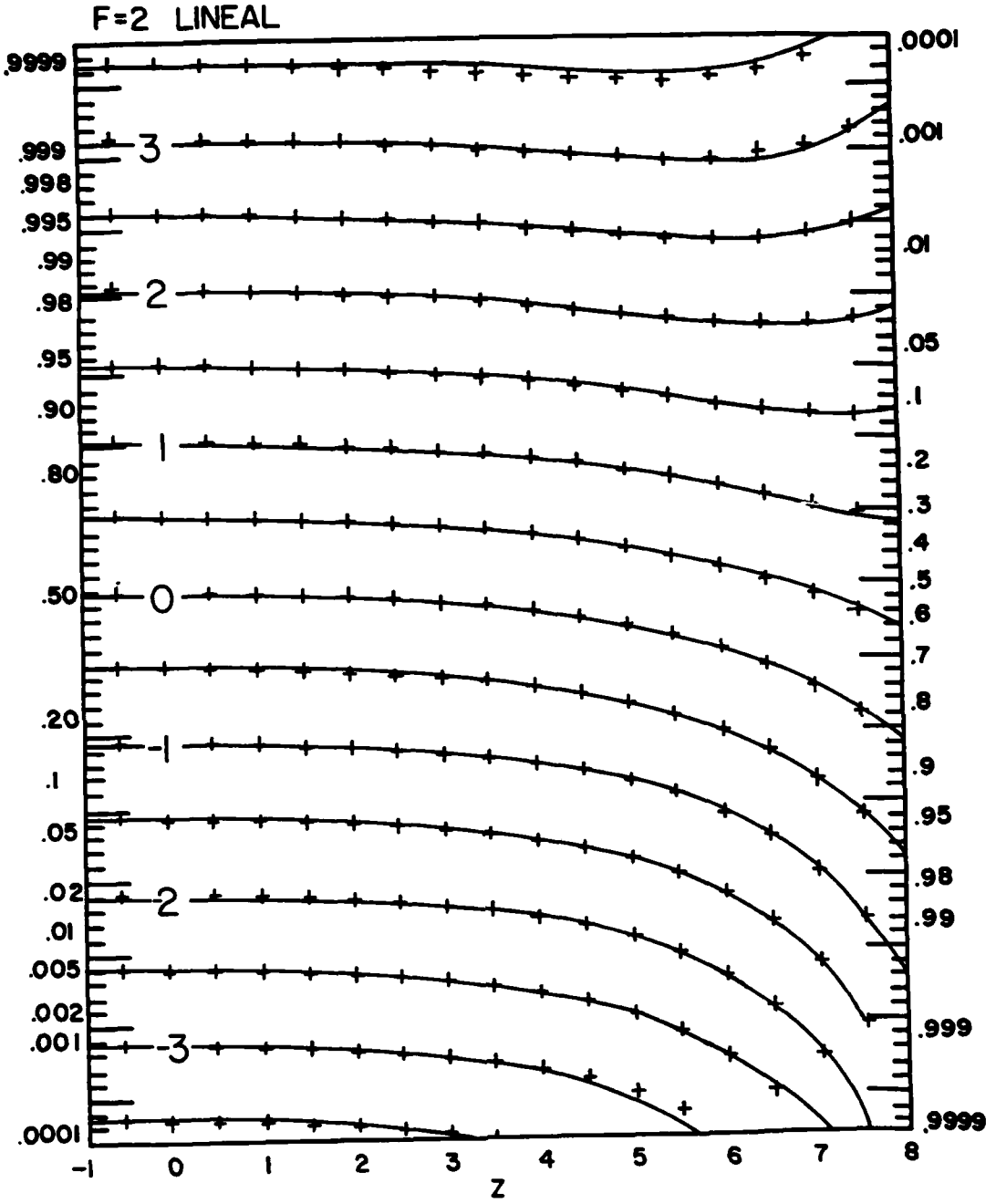

Figure 14. 2/10 or Less Lineal Coverage for Length (s) Corresponding to z = ln s/ln 2. The lines represent the smoothed analyses, each corresponding to a single y_0-value, and the crosses represent the computer solutions

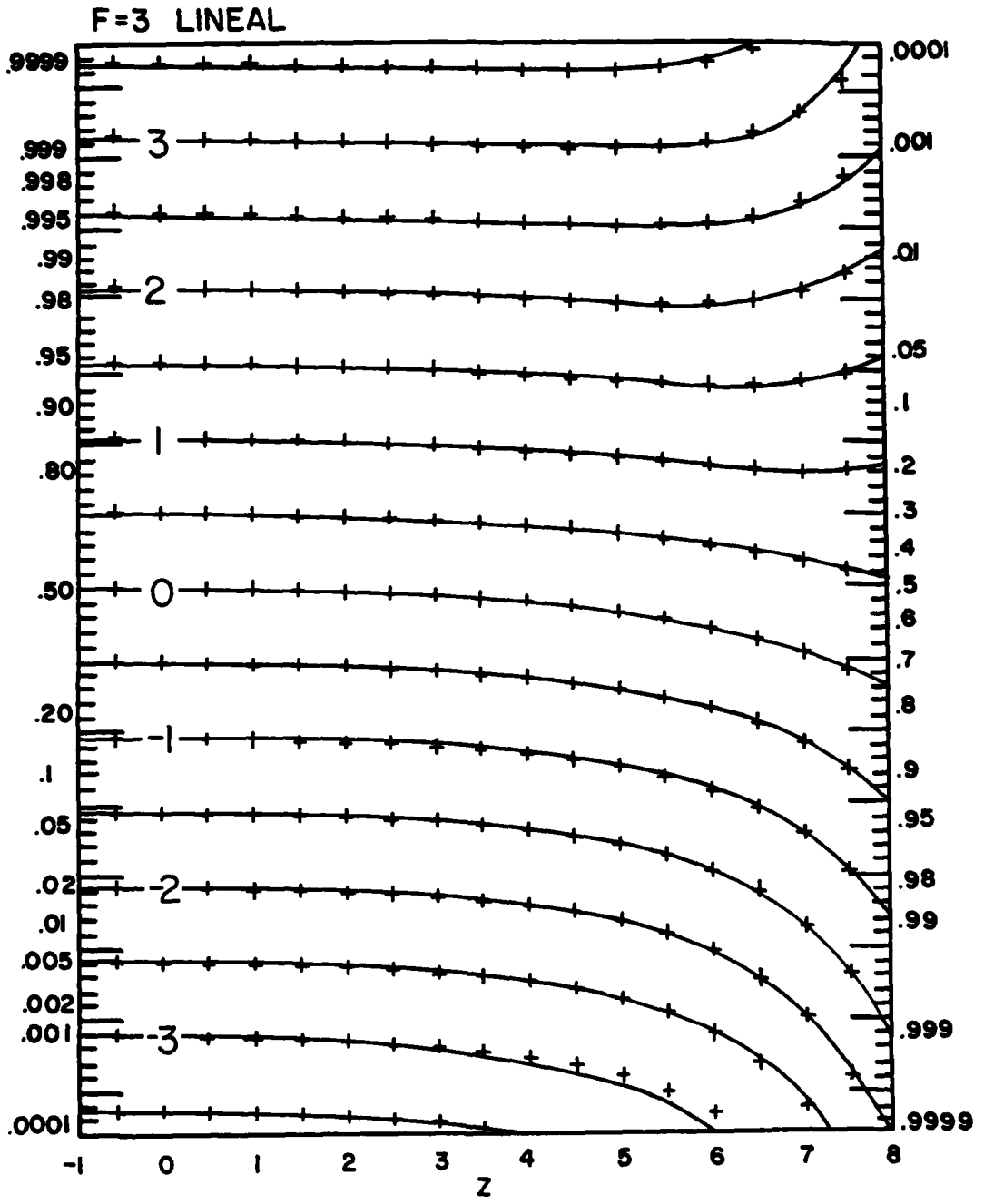

Figure 15. 3/10 or Less Lineal Coverage for Length (s) Corresponding to z = ln s/ln 2. The lines represent the smoothed analyses, each corresponding to a single y_0-value, and the crosses represent the computer solutions

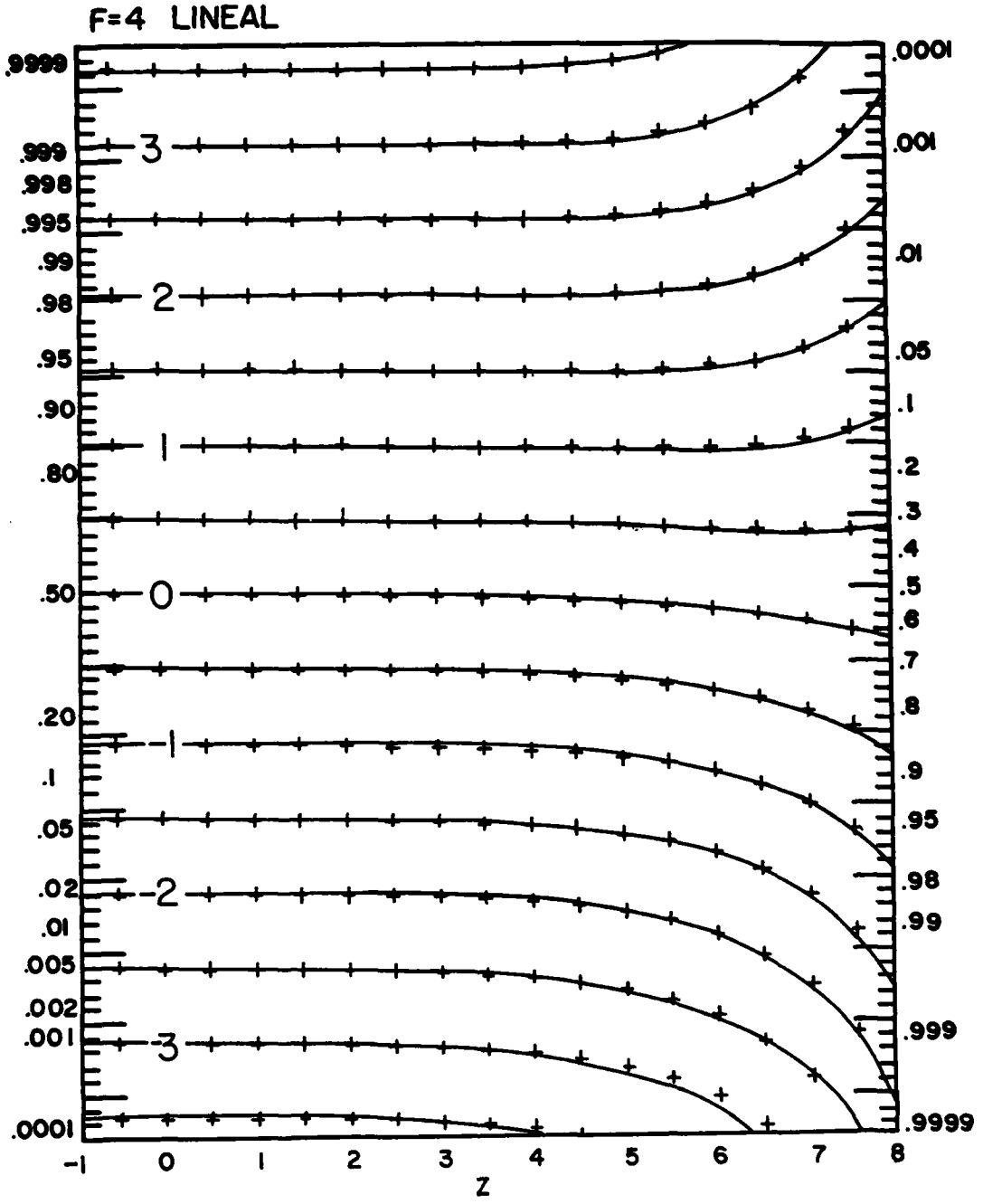

Figure 16. 4/10 or Less Lineal Coverage for Length (s) Corresponding to z = ln s/ln 2. The lines represent the smoothed analyses, each corresponding to a single y_0-value, and the crosses represent the computer solutions

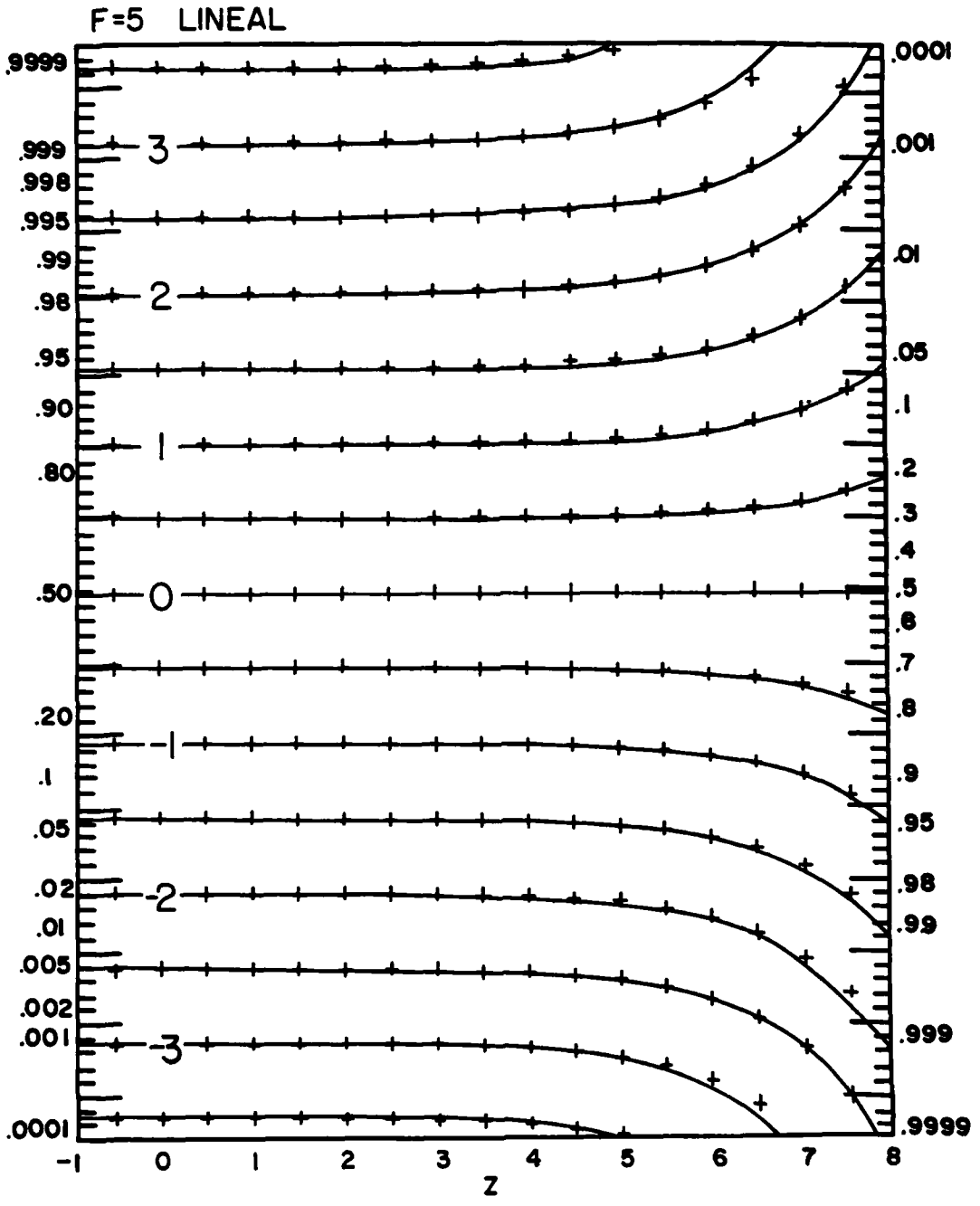

Figure 17. 5/10 or Less Lineal Coverage for Length (s) Corresponding to z = ln s/ln 2. The lines represent the smoothed analyses, each corresponding to a single y_0-value, and the crosses represent the computer solutions

Table 1. Expressions for Each Term of Eq. (8)

Term	Expression	Conditions
α	$y_o + (.006e^{.8z} - .003)(F-5)$	$-1 \le z \le 1.0$
β	$(.9981 + .0011e^{.89z})y_0 + (a_n + b_n e^{c_n z})(F+n-6) - \sum_{i=0}^{n-1}(a_i+b_i e^{c_i z})$ $n = 5 - INT(F)$	$1.0 < z \le 7$
γ	$(.0017e^{.95z} - .3129)(.75 - .3y_o)(1 - .25F)$	$5.5 \le z \le 7$ and $0 \le F \le 4$ and $y_o \ge 2.5$
δ	$\sum_{j=1}^{m}(d(F)_j + f(F)_j e^{g(F)_j y_o})R_j + y'(z=7)$ $R_j = z-7$ (when $m = 1$) $= .5$ ($m = 2$ and $j = 1$) $= z-7.5$ ($m = 2$ and $j = 2$) $m = INT(z-5.5)$ $d(F)_j = -d(F)_j$ $f(F)_j = -f(F)_j$ $g(F)_j = -g(F)_j$ } ($F=5$ and $y_o < 0$)	$7.0 < z \le 8.0$

Table 2. Constants for Eq. (8) (With Table 3)

n	a_n	b_n	c_n
0	.0000	.0000	.00
1	-.0071	.0086	.53
2	-.0205	.0097	.52
3	.0229	.0045	.64
4	-.0517	.0224	.45
5	.0260	.0087	.71

Table 3. Constants for Eq. (8) (With Table 2)

	m = 1			m = 2		
F	$d(F)_m$	$f(F)_m$	$g(F)_m$	$d(F)_m$	$f(F)_m$	$g(F)_m$
0	0.1420	-2.4090	-.44	0.1908	-3.8406	-.56
1	1.0686	-2.2854	-.46	1.8710	-4.2412	-.55
2	1.9440	-2.7842	-.41	3.0540	-4.4752	-.39
3	2.2560	-2.7356	-.40	3.3960	-4.5228	-.50
4	2.0328	-2.2910	-.41	2.0690	-2.5702	-.75
5	1.2356	-1.2300	-1.30	1.6124	-1.5434	-1.51

Table 4. Expressions for Terms of Eq. (9)

$$\eta_i = A + By_o + Cy_o^2$$

$A = a_n + b_n e^{c_n z}$ $\quad C = h_n + q_n e^{r_n z}$ $\quad z > 6$

$B = d_n + f_n e^{g_n z}$ $\quad = 0$ $\quad z \le 6$

$n = \mathrm{INT}(F)$ for $i = 1$

$n = \mathrm{INT}(F) + 1$ for $i = 2$

Table 5. Constants for Eq. (9)

n	a_n	b_n	c_n	d_n	f_n	g_n	h_n	q_n	r_n
0	.0300	-.0366	.51	1.0049	7.44×10^{-4}	.82	8.06×10^{-3}	-1.44×10^{-5}	1.02
1	.0346	-.0366	.47	1.0034	5.08×10^{-4}	.87	1.89×10^{-3}	-3.77×10^{-7}	1.46
2	.0272	-.0283	.46	1.0054	2.77×10^{-4}	.95	2.69×10^{-3}	-2.48×10^{-8}	1.81
3	.0207	-.0213	.44	1.0058	2.74×10^{-4}	.95	-8.76×10^{-4}	-2.34×10^{-12}	2.93
4	.0096	-.0103	.44	1.0021	3.72×10^{-4}	.91	-2.04×10^{-3}	-7.21×10^{-17}	4.17
5	.0000	.0000	.00	1.0022	3.53×10^{-4}	.92	.0000	.0000	0.00

(which are only approximations to the true solutions) and the formula values is no greater than the human error that can be expected from reading the graphs.

This conclusion is confirmed objectively by the root mean square (rms) errors calculated in ENDs between the computer solutions and the Monte Carlo values at intervals of z = -1(1)8. The rms error was broken down by z because, as a whole, Eqs. (8) and (9) do better for small z than for large z. The results are shown in Table 6. For the most part, the rms errors are small, less than 0.03. However, even the largest rms error of 0.100 at z = 8 areal is not too large for our purposes, since the benefits of using the automated method far outweigh the slow, error-prone process of reading from graphs. The extra crosses of Figures 7 and 13 are the empirical solutions to the curves for y_0 = 0.75, 1.25, and 1.75. These results show that Eqs. (8) and (9) not only fit the curves well, but also do a good job of interpolation.

Table 6. Root Mean Square Errors (rmse) Between the Computer Solutions and Analyses, Calculated in END Values

z	-1	0	1	2	3	4	5	6	7	8
rmse (areal)	.000	.008	.015	.016	.017	.024	.028	.045	.066	.100
rmse (lineal)	.012	.011	.011	.015	.016	.019	.021	.026	.028	.019

7. APPLICATIONS

The single-point probability (P_0) and the corresponding END (y_0) of a weather element (X) is easily obtained or estimated from the climatic records, either through equations or graphs, as explained in Section 2. In all applications, it is assumed that such single-point information is available as input.

Two types of application are recognized. In one type, the purpose is to find the probability of the fraction (F) of areal or lineal coverage. The input information in this case consists of the single-point probability (P_0), the areal size (A km^2) or the line length (s' km), and the parameter, scale distance (r km). In the other type of application, the parameter size (r km) must be determined, given, this time, the probability of the fraction (F) of areal coverage for the given area (A) as well as the single-point probability (P_0). By computer, a step-by-step procedure for the first problem is given in Appendix B, and, for the second problem, in Appendix C.

For the model to be effective, the scale distance should be conservative or stable. Thus, it is important that the area or line under consideration be limited

to a region where the spatial correlation is uniformly stable, dependent upon the separation of stations. Otherwise, r will vary, and a single z-value will not be truly representative of a particular line or area. Since r is the distance over which $\rho \stackrel{\cong}{} 0.99$ (when $\Lambda = 340$), an increase in r indicates an increase in the horizontal persistence of a weather element. Seasonally, for clouds and precipitation, r is largest in winter and smallest in summer; diurnally, it is largest around midnight and smallest around midday. In practice, for these elements, r ranges from about 0.5 to 10 km. If r = 0.5 km, then z = 5 corresponds to a square area (or line segment in the linear case) whose side is 16 km, and z = 8 corresponds to an area whose side is 128 km. If r = 10 km, z = 5 represents an area of $(320 \text{ km})^2$, and z = 8 an area of $(2,560 \text{ km})^2$.

The graphs (Figures 6-17) can be used to provide the probability of exceeding a threshold value x in an area or along a line segment. In other words, the 0/10 areal graph (F = 0) gives the probability of exceeding x nowhere in A, the 1/10 areal graph (F = 1) gives the probability of exceeding x in no more than 10 percent of A, and so on. The last graph of the areal series (F = 10) is best understood in terms of the complementary probability, that is, the probability of exceeding x everywhere in A.

7.1 Example for Determining the Probability of a Fraction of Areal Coverage

Let us say that the cumulative probability of 10 mm of rain in 24 hours over a certain rain gauge (in other words, the single-point probability of experiencing an event of 10 mm of rain or less) is P_0'. Suppose r is also given. What is the probability that an entire area (A) surrounding the rain gauge will have a maximum rainfall of 10 mm? Here we have a problem involving the probability of exceeding x (10 mm of rainfall) nowhere in A, and thus the 0/10 areal graph is used (Figure 6b). The values for A and r define the value for z.

To solve the problem graphically, convert P_0' to its corresponding END value (y_0) and follow the appropriate y_0 curve to its intersection with the z-value. The probability P is read on the left-hand scale. (See the example at the end of Section 5). Suppose, for example, $P_0' = 0.31$. The corresponding END value is $y_0 = -0.5$. Further, suppose r = 10 km and $A = 102,000 \text{ km}^2$, yielding z = 5. Then, using Figure 6b, find the intersection of the curve $y_0 = -0.5$ with z = 5. From that point, move leftward, parallel with the z-axis, until the intersection with the END scale is reached. The answer is the P value at that intersection, in this case, 0.080. Therefore, the probability that the 24-hour rainfall will not exceed 10 mm anywhere in A is less than the probability that it will not be exceeded at the rain gauge only, or, in other words, the probability that a rainfall amount somehwere in A will exceed 10 mm increases as A increases. When

using Eq. (8) (Appendix B) to find the solution, set r = 10 km, A = 102,000 km^2, P_0' = 0.31 and F = 0. The answer will be y' = -1.39, for which P(y; F, z) = 0.083. 0.083.

Continuing with this example, what is the probability that the maximum rainfall will be 10 mm in 40 percent of A? Now the problem is the probability of exceeding 10 mm of rainfall in 60 percent of A. Thus, F = 6, and the graph of 4/10 areal coverage (Figure 10) will be used, since, as described earlier, it is the inverted mirror image of the 6/10 areal graph. Therefore, find the intersection of the curve $-y_0$ (for this example, 0.5) with z = 5, and move leftward to intersect the P-scale. The answer is P = 0.66, which corresponds to $P(y_0;F, z)$ = 1-0.66 = 0.34. Using Eq. (8), simply set r = 10, A = 102,000 km^2, P_0' = 0.69, and F = 4. The equation will give a probability of 0.66, and the answer is 1-0.66 = 0.34. Appendix B is written to accept P ' = 0.31, F = 6 and yield probability directly.

The illustrations so far have been to find probability, given y_0, F, and z. In these cases, the use of Eqs. (8) and (9) is fairly straightforward, requiring only simple computer programming. The solutions are unique and can be calculated directly by simply plugging in the appropriate values. There are times, however, when it will be necessary to calculate z, given P_0', F, and $P(y_0; F, z)$, such as in the case of determining the scale distance. Two difficulties arise here because Eqs. (8) and (9) are nonlinear in z. First, z cannot be solved directly by these equations, but must be approximated using iterative methods. Secondly, instead of the solution for z being unique in all cases, there are cases where two solutions or no solution can exist. Let us look more closely at each of these difficulties.

The first difficulty is simple to overcome because many numerical methods already exist for approximating solutions to a high degree of accuracy. They should be available from any good textbook on numerical analysis. Appendix C describes a separate computer program or subroutine to compute z.

The second difficulty can be illustrated graphically by looking at Figure 7. Suppose y_0 = 2. It is easy to see by the shape of this y_0-curve that $P(y_0; F, z)$ can be such that two, or one, or no solution in z exists. Most of the time, however, there will be a unique solution. When there is not, then the procedure (Appendix C) can be made to yield the first, and smaller, estimate of z. Generally, it will be advisable to base a single estimate of z on the average of several algorithmic solutions for z. The final value of r should be based on the average of the z-values. Alternatively, the final value of r may be calculated by determining an r for each of the algorithmic solutions of z and taking the geometric mean of the r-values. Both methods yield identical answers.

7.2 Example for Determining Scale Distance, r

To illustrate the procedure for calculating r, we take an example from Gringorten,[6] and make appropriate changes for converting to the BSW-model and the computer solutions. The monthly publication Hourly Precipitation Data of the National Climatic Center lists nearly 100 stations in New England that report precipitation amounts hourly. We limited the study to these stations, and surveyed the rainfall data for the maximum 24-hour totals for all stations for 21 Januaries (1952-72). We sorted the maxima to obtain estimates of the cumulative probability distribution (P_m). Six widely scattered stations (Burlington, Vt.; Caribou, Me.; Boston, Mass.; Portland, Me.; Hartford, Conn.; Pittsfield, Mass.) were used to establish the single-point cumulative climatic probability distribution (P_c). The climatic frequencies are assumed uniform throughout New England for the purpose of this exercise, and P_c represents the single-point probability.

The estimate of the scale distance for New England precipitation in January was made by using Eq. (7a) to calculate a scale distance ($\hat{r}$) for each of eight thresholds of precipitation, and then taking the geometric mean of those values to obtain r. Since the area of New England is already known ($A = 172,294\,km^2$), we only need to find z for each precipitation category in order to use Eq. (7a). This is done using the present model. We found the frequency of the maximum precipitation amounts that were exceeded nowhere in the given area. Thus, $F = 0$, and, since this is the areal case, we use Figure 6b. As already mentioned, P_c represents the single-point probability; therefore, the END value y_c corresponds to y_0 in the model. P_m represents the probability for the area under question, and corresponds to the $P(y_0; F, z)$ of the model, meaning $y_m = y'$. Thus, the intersection of the y_c-curve with $P = 0.128$ locates the appropriate z-value. For example, for the first precipitation threshold, "none or trace," $P_c = 0.639$, which becomes $y_c = 0.36$, and $P_m = 0.128$. Going now to Figure 6b, find P_m on the left-hand scale and move toward the right, parallel to the z-axis, until the intersection with the appropriate curve for y_c is met. This intersection occurs at $z = 6.0$. Plugging $z = 6.0$ and $\sqrt{A} = 415.1\,km$ into Eq. (7a), we obtain $r = 6.49\,km$. Using the automated method (Appendix C), when we set $P_0' = 0.639$, $P_m = 0.128$, $A = 172,294\,km^2$, and $F = 0$, we obtain $z = 6.01$ and thus $r = 6.44\,km$.

Table 7 gives the results of applying Appendix C to the New England January 24-hour precipitation for each of the eight thresholds of rainfall amount. The table shows the single-point climatic frequency and the frequency of the maximum in each of four areas of increasing size, and the resulting estimates of scale distance. The estimates vary widely, as might be expected, because of the collective nature of the rainfall data for areal coverage. Nevertheless, the mean

Table 7. New England January 24-h Precipitation Frequency Distributions (P_0') at a Single Station and the Frequency Distribution (P) of the Maximum 24-h Precipitation in Successively Larger Areas, With Resulting Estimates of the Parameter: Scale Distance (r km)

Amt (mm)	Point Frequency P_0'	Area 1 21,358 km^2 P	$\hat{r}$	Area 2 37,455 km^2 P	$\hat{r}$	Area 3 86,377 km^2 P	$\hat{r}$	Area 4 172,294 km^2 P	$\hat{r}$
≤ Trace	.639	.389 (.398)	6.44	.362 (.335)	7.46	.161 (.223)	5.28	.128 (.127)	6.44
≤ 2.5	.787	.583 (.582)	6.69	.564 (.520)	8.04	.400 (.399)	6.72	.359 (.274)	8.38
≤ 5	.853	.720 (.683)	8.32	.704 (.628)	9.98	.586 (.514)	8.32	.545 (.386)	10.35
≤ 10	.921	.802 (.805)	6.44	.786 (.765)	7.52	.724 (.675)	8.02	.692 (.563)	9.99
≤ 15	.954	.856 (.875)	5.37	.844 (.846)	6.29	.801 (.779)	7.40	.776 (.691)	9.22
≤ 20	.973	.9008 (.9205)	4.89	.888 (.900)	5.66	.855 (.852)	6.72	.836 (.787)	8.38
≤ 25	.989	.9253 (.964)	3.14	.9192 (.954)	3.86	.9023 (.929)	4.88	.890 (.893)	6.22
≤ 50	.9989	.9914 (.9953)	3.57	.9883 (.9940)	3.98	.9821 (.9906)	4.09	.9791 (.9848)	5.22

Overall geometric mean $\hat{r}$ = 6.37 km

The bracketed figures are the probability estimates based on a single estimation of the scale distance: 6.37 km.

(geometric) of all the scale distances, r = 6.37 km, when used with Appendix B, yielded the probability estimates shown in the brackets (Table 7). The 100-station frequencies are plotted in Figure 18 at the X's, and the BSW-model probabilities are shown by the curves for the eight maxima of precipitation.

If the results, by the model, are viewed as smoothed corrections to the frequencies provided by the data, then one or two surmises might be made. The probability of no rain in an area is well estimated by a 21-year survey of some hundred stations in New England. The probability of light or moderate rainfall (2.5 - 20 mm), however, tends to be underestimated by the records, suggesting that greater maxima would have been obtained if there had been more reporting stations. On the other hand, the heavy precipitation, such as 1 or 2 inches (25 or 50 mm) of rain, corresponding to 10 or 20 inches of snowfall, might have occurred a little more frequently than expected in the 21 Januaries of the record.

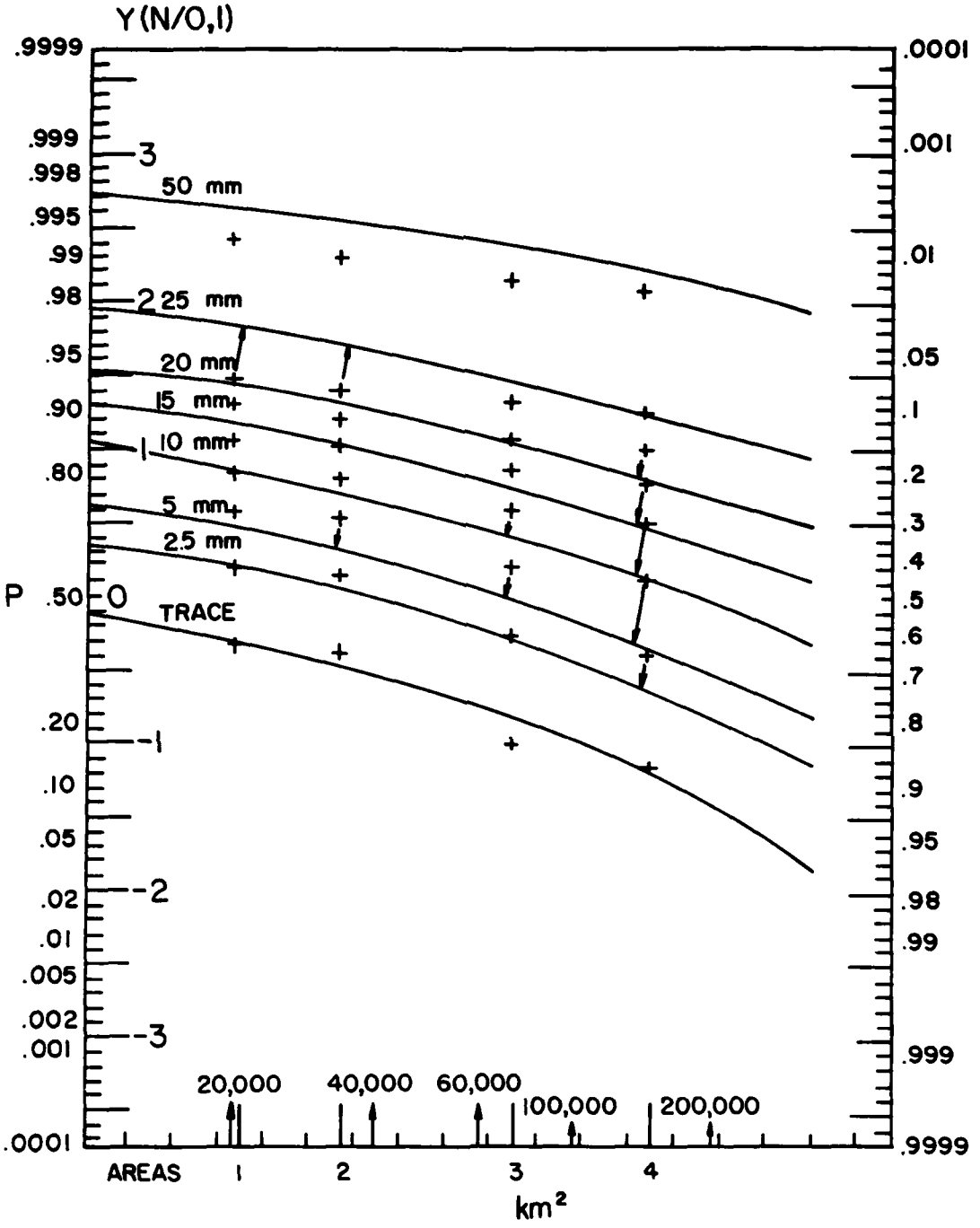

Figure 18. The Plot of the Data of Table 7: Probabilities of Maximum 24-h precipitation in an Area Versus Areal Extent

In all of New England, precipitation exceeding 2 inches occurred on 13 days to give the 2 percent frequency. The model estimates 1.5 percent frequency, or nine such days in January in a 21-year period. The large scale distance (r = 6.37 km) indicates that New England winter precipitation patterns have strong horizontal persistence, as you would expect.

7.3 Modeling Areal and Lineal Cloud Cover

We present an example of areal and lineal cloud cover to illustrate the model application with respect to fractional cloud cover. Initially, we must make two important assumptions. First, we adopt the mean sky-cover as the probability of a cloud presence vertically above a single point (P_0). The no-cloud probability then becomes $P_0' = 1 - P_0$. Second, we assume that the celestial dome, as seen by the weather observer, has a radius of 27.8 km. This translates into a floor space of area A = 2424 km^2.

Table 8. Cloud-Cover Statistics at Bedford, Mass., January, 1200-1400 LST, Based on RUSSWO Data of 1946-1967

RUSSWO Data		Cumulative		
Sky Cover	Frequency	Sky Cover	Frequency	$\hat{z}$
Clear	.155	0.5	.155	4.64
1	.043	1.5	.198	4.82
2	.049	2.5	.247	4.62
3	.041	3.5	.288	4.39
4	.041	4.5	.329	3.29
5	.031	5.5	.360	NA
6	.027	6.5	.387	4.87
7	.044	7.5	.431	4.85
8	.060	8.5	.491	4.92
9	.046	9.5	.537	4.50
Overcast	.462	$\bar{z}$ = 4.54	r = 2.11 km	

Table 8 shows, in the first column, the climatic summary of the frequency of cloud cover for Bedford, Mass., January 1200-1400 LST, as taken from the Revised Uniform Summaries of Surface Weather Observations (RUSSWO). RUSSWOs are prepared by the USAF Environmental Technical Applications Center. They report the observations of total sky cover in tenths, from clear to overcast, and show the percentage frequency of each tenth. These values represent an average of the three hourly frequencies (1200, 1300, and 1400 LST). We converted the data into cumulative frequencies, as shown in the third and fourth columns of Table 8. To do this, we assumed that the categories of tenths represent equal intervals, such that 0 tenths includes all cases from 0 to 0.5 tenths, 1 tenth all cases from 0.05 to 1.5 tenths, and so on, until, lastly, 10 tenths includes all cases from 9.5 tenths to 10 tenths. From the RUSSWO, we obtain the mean sky cover, $P_0 = 0.66$, and $P_0' = 1 - 0.66 = 0.34$.

We now have enough information to calculate z-values. For example, the third row of Table 8 gives $F = 2.5$ and $P(y_0; F, z) = 0.247$. With $P_0' = 0.34$, using Appendix C, we obtain $\hat{z} = 4.62$. We calculated the z-values for each category of cumulative frequency (Table 8). We then estimated the mean z-value as $\bar{z} = 4.54$. Using Eq. (7), with $A = 2424\,km^2$, we obtain $r = 2.11\,km$. With the scale distance and Appendix B, we can now make the model estimates of the fractional cover. Table 9 shows these estimates in the middle column for comparison with the RUSSWO frequencies. The rms difference between the sets of values is 0.015. The solid curve labeled "sky dome" in Figure 19 is the BSW model estimate, and the X's are plots of the RUSSWO data.

The model can be used, further, to obtain the probability distribution of fractional cover for areas both smaller and larger than the celestial dome. The first column of Table 9 shows the estimates for a small area ($100\,km^2$), revealing that the likelihood of all-clear (left-hand scale) of Figure 19 and full-overcast (right-hand scale) increases, and the likelihood of partical cover decreases. For a much larger area, $100,000\,km^2$ (third column, Table 9), the reverse is true. Figure 19 illustrates that the likelihood of all-clear and overcast vanishes with increasing floor space. Similar results are obtained for cloud presence along a line of travel (Table 10), using Appendix B and the same Bedford, Mass., data (January 1200-1400 LST).

8. SUMMARY AND CONCLUSIONS

Empirical equations were developed for determining the probabilities of areal and lineal coverages of weather conditions, making it possible to obtain solutions quickly from a computer. Point probabilities of weather conditions

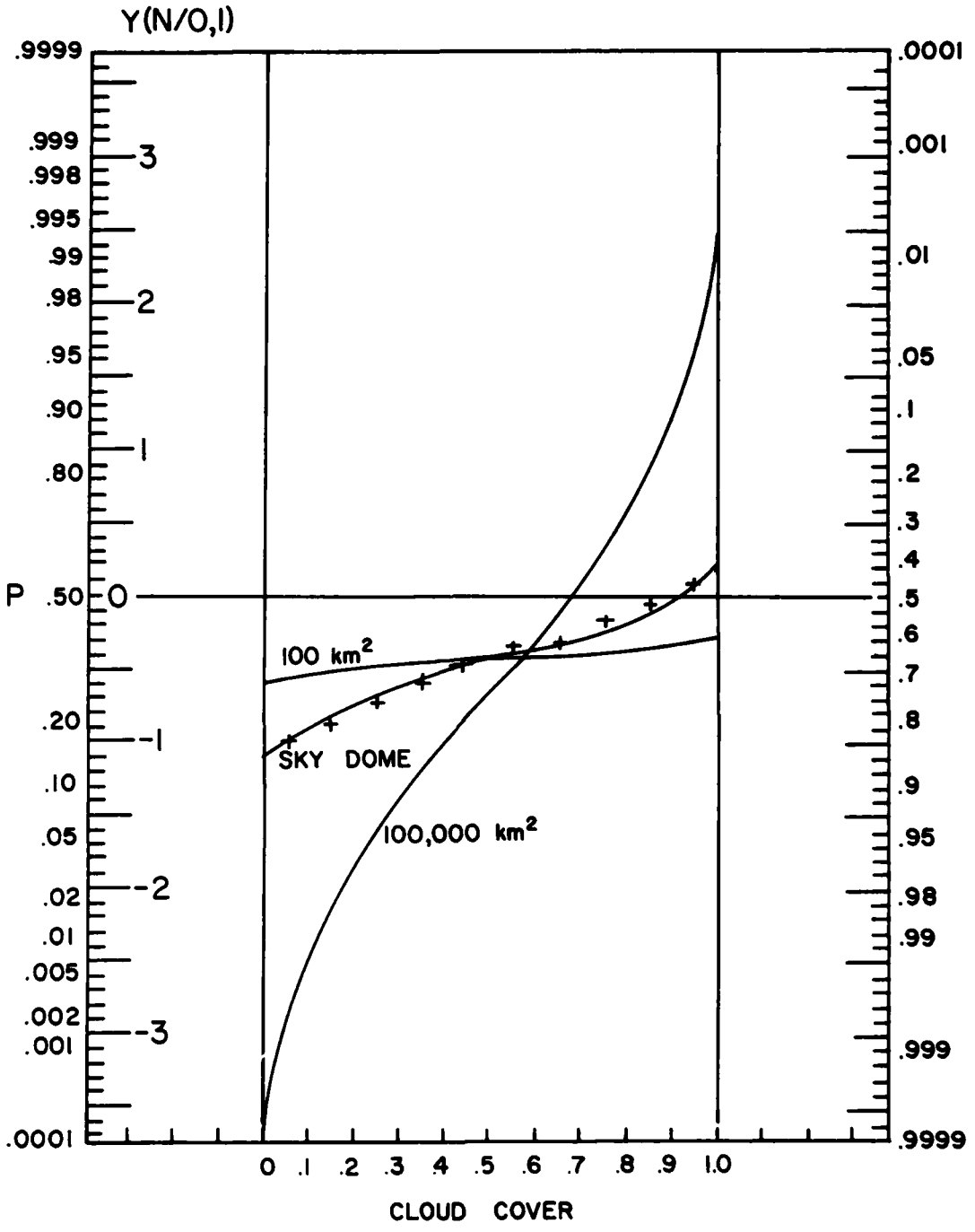

Figure 19. Total Cloud Cover at Bedford, Mass., January, 1200-1400 LST

Table 9. BSW-Model Probability Estimates of the Cloud Cover, as a Function of the Floor Area, for Bedford, Mass., January, 1200-1400 LST, Compared With Table 8

Sky Cover (Tenths)	Cumulative Frequencies		
	$100\,km^2$	$2424\,km^2$ (Celestial dome)	$100,000\,km^2$
0.5	.298	.170	.001
1.5	.312	.220	.015
2.5	.321	.255	.051
3.5	.330	.286	.121
4.5	.336	.316	.215
5.5	.344	.348	.313
6.5	.350	.380	.459
7.5	.359	.417	.640
8.5	.369	.461	.815
9.5	.384	.534	.978
Overcast	.616	.466	.022
RMSD		.015	
BIAS		.013	

were extended to lines and areas by means of Monte Carlo simulation. The Boehm Sawtooth Wave (BSW) model was used in the simulation procedure because it is simple, fast, and has a realistic spatial-correlation function. The procedure was to use the model to generate 25,000 maps for each of twelve different-sized square areas and lines. Subsequently, probability distributions were approximated at selected threshold values, and the results were put in graphical form. From these graphs, the empirical solutions were determined.

These results are approximate, depending upon the effectiveness of the BSW, and the degree of accuracy of the Monte Carlo process, the smoothed curves, and the fit of the equations. The final model must be tested over a period of time to determine how well it works and to determine its strengths and weaknesses. One such test would be to measure its ability to tolerate climatic differences within a

Table 10. BSW-Model Probability Estimates of Cloud Presence, Overhead, Along a Line of Travel, for Bedford, Mass., January, 1200-1400 LST

Fraction of line with cloud	Cumulative Frequencies		
	10 km	100 km	500 km
0	.309	.150	.004
.1	.314	.183	.019
.2	.321	.228	.048
.3	.326	.254	.100
.4	.333	.293	.175
.5	.340	.332	.269
.6	.347	.372	.387
.7	.353	.418	.522
.8	.359	.462	.666
.9	.366	.511	.803
1.0	.371	.561	.921
Complete Cover	.629	.439	.079

region. A question to be answered is: To what extent can one scale distance parameter be used before the model will no longer work? This, as well as other questions, will be answered through research, application and experience.

Finally, the challenge still remains to solve the areal and lineal coverage problem analytically. This solution would provide a basis upon which to judge the current results. If the true solution is unduly complicated, and if the current work is reasonably accurate, it might be desirable, or even necessary, to continue to use these results for programming and practical applications.

References

1. Schreiner, L.C., and Riedel, J.F. (1978) Probable maximum precipitation estimates United States east of 105th meridian, Hydrometeorol. Report (No. 51), NOAA-NWS-HR-51.
2. Court, A. (1961) Area-depth rainfall formulas, J. Geophys. Res. 66:1823-1831.
3. Roberts, C.F. (1971) A note on the derivation of a scale measure for precipitation events, Mon. Wea. Rev. 99:873-876.
4. Briggs, J. (1972) Probability of aircraft encounters with heavy rain, Meteorol. Mag. 101:8-13.
5. Jones, D.M.A., and Wendland, W.M. (1983) Statistics of Instantaneous Rainfall Rates, AFGL-TR-83-0056, AD A130089.
6. Gringorten, I.I. (1979) Probability models of weather conditions occupying a line or an area, J. Appl. Meteorol. 18:957-977.
7. Bertoni, E.A., and Lund, I.A. (1964) Winter space correlations of pressure, temperature and density to 16 km, Environ. Res. Papers (No. 75), AFCRL-64-1020, AD 611002.

Appendix A

Derivation of BSW Model Correlation Coefficient

Purpose: To find the correlation coefficient (cc), ρ (s), in the BSW-model as a function of the standardized distance (s) between two points in the field.

Because the equivalent normal deviate (END) has mean zero and variance one, the correlation coefficient (ρ_y) between two END's (y, y') is given by

$$\rho_y = E(yy'). \tag{A1}$$

The correlation coefficient (ρ_x) between the phases (x, x') of a single wave formation, at two randomly selected points, distance (s) apart, is given by

$$\rho_x = \frac{E(xx') - \bar{x}^2}{\sigma_x{}^2} \tag{A2}$$

where E(xx') is the covariance

$\bar{x}$ is the mean, for both x and x', and

σ_x is the standard deviation.

In the BSW-model, $\bar{x} = 1/2$, $\sigma_x^2 = 1/12$.

As given in the text, the result of having N wave formations in the field is to produce N values of x at each point in the field, to give the END (y)

$$y = \frac{\sqrt{N}}{\sigma_x} \left\{ \frac{1}{N} \sum_{i=1}^{N} x_i - \bar{x} \right\}. \tag{A3}$$

Between two points, where the END's are y and y'

$$\rho_y = E(yy') = \frac{N}{\sigma_x^2} \cdot E \left\{ \frac{1}{N} \sum x_i - \bar{x} \right\} \cdot \left\{ \frac{1}{N} \sum x_i' - \bar{x} \right\}$$

$$= \frac{N}{\sigma_x^2} \cdot E \left\{ \frac{1}{N^2} \sum\sum x_i x_j' - \bar{x}^2 \right\}. \tag{A4}$$

But, as seen from Eq. A2 above,

$$E(x_i x_j') = \rho_x \cdot \sigma_x^2 + \bar{x}^2 \quad \text{when } i = j \tag{A5a}$$

and, through independence of the wave formations,

$$E(x_i x_j') = \bar{x}^2 \quad \text{when } i \neq j \tag{A5b}$$

Hence, $$\rho_y = \frac{N}{\sigma_x^2} \cdot \left\{ \frac{1}{N} (\rho_x \sigma_x^2 + \bar{x}^2) + \frac{N-1}{N} \cdot \bar{x}^2 - \bar{x}^2 \right\}$$

which reduces to $\rho_y = \rho_x$ and the following derivation for ρ_x is admissable for ρ_y. (A6)

Without loss of generality, we can let the wavelength (Λ) be the unit distance, and limit the discussion to one formation of waves (Figure A1), oriented east-west, and find the covariance (Exx') between two points separated by distance (s) in the U, V-field.

Corresponding to the two degrees of freedom for each wave formation, we choose the two points by randomly locating the first point along the U-axis at the wave-phase distance (x) from the origin, and the second point on a circle of radius (s), centered on the first point, with random angle (θ) from the U-axis. The limits of variation of x and θ are

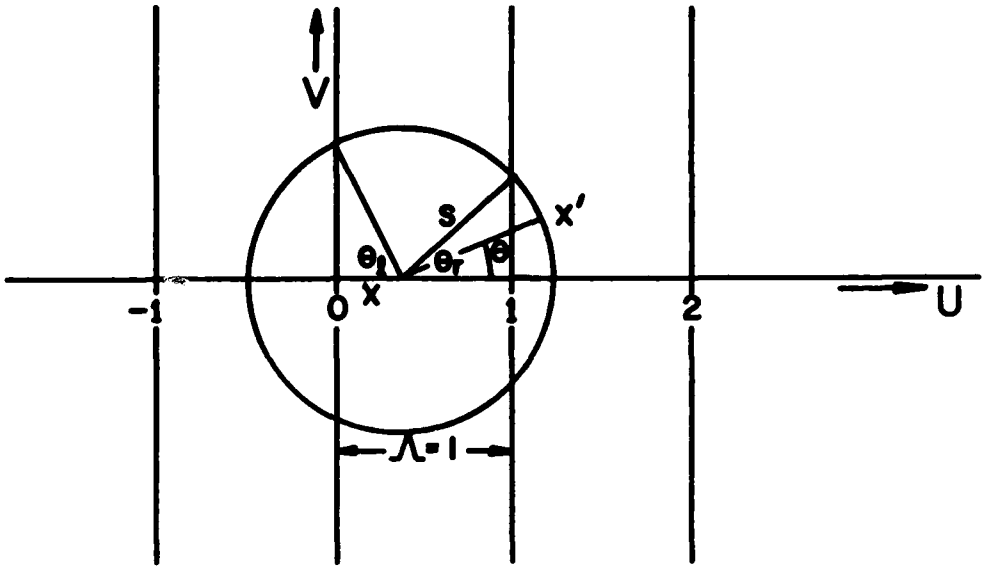

Figure A1. Diagram for Derivation of $\rho(s)$ $0 \leq s \leq 1$

$$0 \leq x \leq 1$$

$$0 \leq \theta \leq \pi . \tag{A7}$$

(Note: While θ should vary from 0 to 2π, the effect on the convariance is repeated in the region $\pi < \theta \leq 2\pi$.)

The wave-phase (x') at the second point is given by

$$x' = x + s \cos \theta + \delta \tag{A8}$$

where $\delta = 0, \pm 1, \pm 2$, etc., depending in which wave the second point is located.

The exercise is now narrowed down to finding an expression for the covariance, E(xx').

Within the prescribed limits of integration

$$E(xx') = \frac{1}{\pi}\int_{x=0}^{1}\int_{\theta=0}^{\pi} x(x+s\cos\theta+\delta)\,dx\,d\theta \qquad (A9)$$

or,
$$\pi.E(xx') = \int_{x=0}^{1}\int_{\theta=0}^{\pi} x^2\,dx\,d\theta + s\int_{x=0}^{1}\int_{\theta=0}^{\pi} x\cos\theta\,dx\,d\theta + \int_{x=0}^{1}\int_{\theta=0}^{\pi} x.\delta\,dx\,d\theta .$$

The first double integral reduces to $\frac{\pi}{3}$; the second, to zero. The third double integral requires careful attention because of the varying values of δ .

So far

$$\pi.E(xx') = \frac{\pi}{3} + \int_{x=0}^{1}\int_{\theta=0}^{\pi} x.\delta\,dx\,d\theta . \qquad (A10)$$

For $0 \le s \le 1$,

$\delta = -1$ for $0 \le \theta \le \theta_r$ where $\theta_r = \cos^{-1}\frac{1-x}{s}$

$= 0$ for $\theta_r < \theta \le \pi - \theta_\ell$ where $\theta_\ell = \cos^{-1}\frac{x}{s}$

$= 1$ for $\pi - \theta_\ell < \theta \le \pi$. .

Hence,

$$\pi.E(xx') = \frac{\pi}{3} + (-1)\int_{x=1-s}^{1} x\,dx\int_{\theta=0}^{\theta_r} d\theta + (1)\int_{x=0}^{s} x\,dx\int_{\theta=\pi-\theta_\ell}^{\pi} d\theta$$

which reduces to

$$\pi . E(xx') = \frac{\pi}{3} - \int_{x=1-s}^{1} x dx \left\{ \cos^{-1} \frac{1-x}{s} \right\} + \int_{x=0}^{s} x dx \left\{ \cos^{-1} \frac{x}{r} \right\}$$

$$= \frac{\pi}{3} - \int_{x=1-s}^{1} (1-x) d(1-x) \left\{ \cos^{-1} \frac{1-x}{s} \right\} + \int_{x=1-s}^{1} d(1-x) . \cos^{-1} \frac{1-x}{s}$$

$$+ \int_{x=0}^{s} x \cos^{-1} \frac{x}{s} dx.$$

Replacing x with z = 1 - x,

$$\pi . E(xx') = \frac{\pi}{3} - \int_{z=s}^{0} z dz \cos^{-1} \frac{z}{s} + \int_{z=s}^{0} dz . \cos^{-1} \frac{z}{s} + \int_{x=0}^{s} x \cos^{-1} \frac{x}{s} dx$$

$$= \frac{\pi}{3} + 2 \int_{x=0}^{s} x \cos^{-1} \frac{x}{s} dx - \int_{x=0}^{s} \cos^{-1} \frac{x}{s} dx.$$

These integrals are readily found in tables of integrals to give, finally

$$\pi . E(xx') = \frac{\pi}{3} + \frac{\pi s^2}{4} - s.$$

Hence, $\rho_x = \dfrac{\left(\dfrac{1}{3} + \dfrac{s^2}{4} - \dfrac{s}{\pi} \right) - \bar{x}^2}{\sigma_x^2}$

and, for the BSW-model,

$$\rho_x = 1 - \frac{12}{\pi} s + 3 s^2. \qquad \text{(A11)}$$

Since this cc is the same for the y-values, and is found in terms of s, we use the symbol $\rho(s)$, and thus

$$\rho(s) = 1 - \frac{12}{\pi} s + 3 s^2.$$

For $1 < s \leq 2$ (see Figure A2),

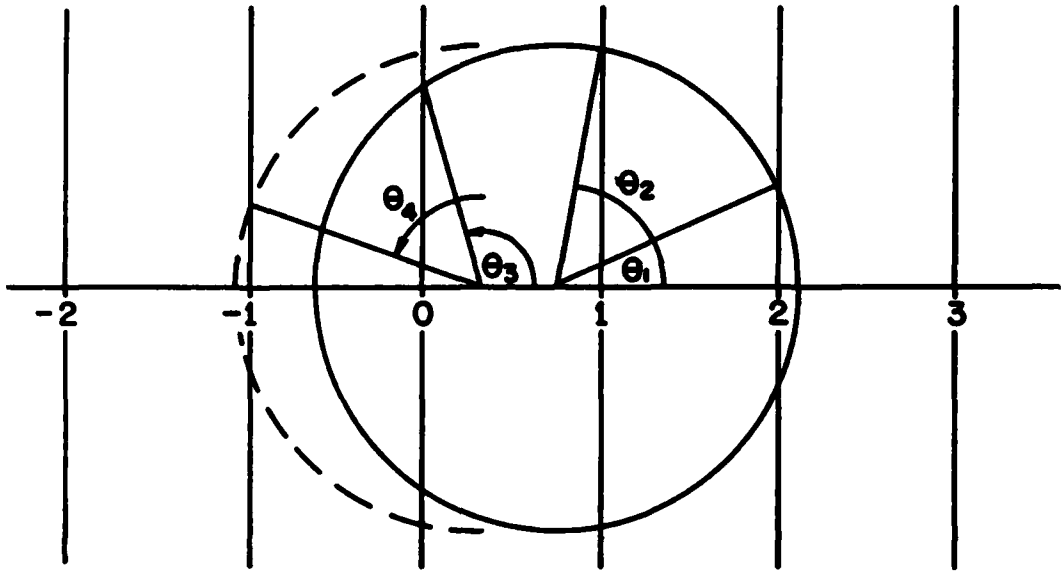

Figure A2. Diagram for Derivation of $\rho(s)$ for $1 < s \leq 2$

$$\delta = -2 \text{ for } 0 \leq \theta < \theta_1 \text{ where } \theta_1 = \cos^{-1} \frac{2-x}{s}$$

$$= -1 \text{ for } \theta_1 \leq \theta < \theta_2 \text{ where } \theta_2 = \cos^{-1} \frac{1-x}{s}$$

$$= 0 \text{ for } \theta_2 \leq \theta < \pi - \theta_3 \text{ where } \theta_3 = \cos^{-1} \frac{x}{s}$$

$$= 1 \text{ for } \pi - \theta_3 \leq \theta < \pi - \theta_4 \text{ where } \theta_4 = \cos^{-1} \frac{1+x}{s}$$

$$= 2 \text{ for } \pi - \theta_4 \leq \theta \leq \pi .$$

Returning to Eq. (A10)

$$\pi . E(xx') = \frac{\pi}{3} + (-2) \int_{x=2-s}^{1} x\,dx \int_{\theta=0}^{\theta_1} d\theta$$

$$+ (-1) \int_{x=2-s}^{1} x\,dx \int_{\theta=\theta_1}^{\theta_2} d\theta + (-1) \int_{x=0}^{2-s} x\,dx \int_{\theta=0}^{\theta_2} d\theta$$

$$+ (\text{terms equal to zero when } \delta = 0)$$

$$+ (1) \int_{x=s-1}^{1} x\,dx \int_{\theta=\pi-\theta_3}^{\pi} d\theta + (1) \int_{x=0}^{s-1} x\,dx \int_{\theta=\pi-\theta_3}^{\pi-\theta_4} d\theta$$

$$+ (2) \int_{x=0}^{s-1} x\,dx \int_{\theta=\pi-\theta_4}^{\pi} d\theta$$

The work involved in solution of these integrals is straightforward but voluminous. The end product is

$$\pi . E(xx') = \frac{\pi}{3} + \frac{\pi}{4} s^2 - s + 2 \left\{ \cos^{-1} \frac{1}{s} - \sqrt{s^2 - 1} \right\}$$

and gives

$$\rho_x = (1 - \frac{12}{\pi} s + 3 s^2) + \frac{24}{\pi} \left\{ \cos^{-1} \frac{1}{s} - \sqrt{s^2 - 1} \right\}$$

which, as before, is symbolized as $\rho(s)$.

In summary,

$$\rho(s) = 1 - \frac{12}{\pi} s + 3 s^2 \quad \text{for } 0 \le s \le 1$$

$$= (1 - \frac{12}{\pi} s + 3 s^2) + \frac{24}{\pi} \left\{ \cos^{-1} \frac{1}{s} - \sqrt{s^2 - 1} \right\} \quad \text{for } 1 < s \le 2.$$

Appendix B

Estimating the Probability of Fractional Coverage by Computer

Problem: By computer, using the BSW-model, find the probability $P(y_o;F,z)$ that a weather condition will be exceeded in no more than a certain fraction of an area or line.

Given: X = threshold value of weather parameter not to be exceeded

P_o' = single-point cumulative probability $(1-P_o)$ of the occurrence of x

A or S' = the area (km^2) or line (km) in question

F/10 = the fraction of A or s' in which X may be exceeded

r = the model parameter, scale distance (km)

Procedure:

Step 1. Calculate the equivalent normal deviate (END) (y_o) of P_o' using the National Bureau of Standards (NBS) formula as follows:

$$y_o = k\left(t - \frac{a_o + a_1 t}{1+b_1 t+b_2 t^2}\right) + \epsilon \qquad \text{(B1)}$$

where $k = -1$, $t = \sqrt{\ell n \frac{1}{(P_o')^2}}$ when $P_o' \leq 1/2$

$$k = 1,\ t = \sqrt{\ell n \frac{1}{(1-P_o')^2}} \qquad \text{when } P_o' > 1/2$$

$$|\epsilon| < .003$$

$$a_o = 2.30753 \qquad b_1 = .99229$$

$$a_1 = .27061 \qquad b_2 = .04481$$

Step 2. Calculate z by entering $\sqrt{A}$ or S' and r into Eq. (6).

Step 3. Enter y_o, F, and z into Eq. (8) for the areal case and Eq. (9) for the lineal case. The expressions, conditions, and constants for these equations are shown in Tables 1-5, as explained in Section 6. The answer will be given in terms of the END value, y'.

Step 4. Calculate $P(y_o;F,z)$ using the NBS formula as follows:

$$P(y_o;F,z) = \ell + m\left(\frac{1}{2(1+c_1|y'|+c_2y'^2+c_3|y'|^3+c_4y'^4)^4}\right) + \epsilon \qquad \text{(B2)}$$

where $\ell = 0,\ m = 1$ for $y' < 0$

$\ell = 1,\ m = -1$ for $y' \geq 0$

$|\epsilon| < .00025$

$C_1 = .196854 \qquad C_3 = .000344$

$C_2 = .115194 \qquad C_4 = .019527$

Appendix C

Estimating Scale Distance by Computer

Problem: By computer, using the BSW-model, compute the parameter, scale distance (r km).

Given: X = threshold value of weather parameter not to be exceeded

P_o' = single-point cumulative probability ($1-P_o$) of the occurrence of x

A = the area (km^2) in question

F/10 = the fraction of A in which X may be exceeded

$P(y_o;F,z)$ = the probability that x will be exceeded in no more than F/10 of A

Discussion: Eq. (8) was derived to solve for $P(y_o;F,z)$ given P_o', A, F and r (see Appendix B). To find r when it is the unknown, a system of trial and error is used. The equations in Table 1 are given in terms of z, which has a one-to-one relation with r when A is known. The procedure, then, is to begin with the trial z-value of $z_i = -1$, and increase z_i gradually in stages of Δz until an accurate estimate of the correct z-value is found. The smaller Δz is, the smaller the error (ϵ) will be for the estimate of z where $|\epsilon| < \Delta z$. If there are two solutions for z, this procedure will yield the lesser value (see Section 7). Other iterative methods, available from any good textbook on numerical analysis, may be used as well.

Procedure:

Step 1. Calculate the equivalent normal deviate (END) (y_o) of P_o' using the

National Bureau of Standards (NBS) formula [Appendix B, Eq. (B1)].

Step 2. Calculate the END (y') of $P(y_o;F,z)$ using the NBS formula.

Step 3. Initialize $z_i = -1$ and Δz.

Step 4. Enter y_o, F, and z_i into Eq. (8). The expressions, conditions, and constants for this equation are shown in Tables 1-3, as explained in Section 6. The answer will be an interim value y_I' that is to be compared with y'.

Step 5. Calculate $\Delta y' = y' - y_I'$.

Step 6. Increase z_i by Δz and return to Step 4 until $\Delta y'$ becomes negative, or until $z_i = 8$.

Step 7. If $\Delta y'$ is negative, z is estimated by

$$z = z_i - \left(\frac{y' - y_I(z_i)}{y_I(z_i - \Delta z) - y_I(z_i)} \right) \Delta z + \epsilon \text{, where } |\epsilon| < \Delta z.$$

If $\Delta y' = 0$, $z_i = z$. If $z_i = 8$, there is no solution within the bounds of the graphs.

Step 8. Enter z and $\sqrt{A} = s'$ into Eq. (7) to obtain the estimate for r.


FILM